Capturing More Light:

Phycobilisomes Characterization for

Increased Hydrogen Production Efficiency

A Thesis Presented for the

Master of Science

Degree

The University of Tennessee, Knoxville

Paul Abraham Willard

May 2012

Dedicated to my parents

Acknowledgements

First and foremost, I would like to thank my PI, Dr. Barry Bruce, for letting me work in his lab. I joined his lab as an undergrad. After graduating with my B.S., he offered to hire me as a tech. Barry has been patient, and has helped me with advice and ideas when needed. I have always admired his passion for the work done in his lab, which in turn, has inspired me to pursue this work. Dr. Frymier has also been a great mentor to work with and talk to both inside and outside the lab. Also, I would like to thank Dr. Boder for agreeing to be on my committee, and for helping guide me through graduate school.

Much thanks goes out to Michael Vaughn, a former lab mate, who helped to get me started on my work with phycobilisomes. Prakitchai "Non" Chotewutmontri has also given me much advice over the years with regards to everyday lab work. Thanks to Danielle Williams, too, who helped a lot with culturing of the cyanobacteria with which I worked.

A special thank you goes out to my friend, Andrew Herget, who is no longer with us. Barry let him work with me in the lab for two semesters. Andrew was a good friend, both inside and outside the lab, and he always managed to get the work assigned to him done.

I want to thanks Tihami Qureshi for her support and encouragement. She has been a tremendous help and always managed to keep my spirits high. I want to thank my parents for always supporting me and offering to help in any way they could.

Abstract

Alternative energy and biofuels are a growing area of research. The demand for more and clean energy is ever increasing, but the current technology is inefficient, expensive, and incapable of meeting the demands of the current market. Hydrogen is a potential future fuel, as it is both clean and renewable, but its formation through conventional means is costly and inefficient. Photosynthesis can be utilized for the formation of hydrogen, which can then serve as a convenient and renewable biofuel. Photosynthetic hydrogen evolution is observed *in vitro*, but the current photosystem design is not very versatile and optimized to use all incident light it may receive from the sun. Manipulating the photosynthetic machinery by adding phycobilisomes, light-absorbing antennae, to the *in vitro* system, can potentially boost the absorption and utilization of light available to this system.

To make use of phycobilisomes in this system, a careful look at the structural stability and dissociation pathway of the complex into smaller pieces is pursued to isolate the desired phycobilisome rod component. These rod components are ideal for utilization because of their natural ability to transfer energy to the photosystem, but the organisms from which they are isolated do not preferentially produce them. In addition, a mechanism by which phycobilisome rods can attach to the designed hydrogen evolving system and the completed preparative molecular biology work is presented.

Table of Contents

Chapter 1: Phycobilisomes **1**

1. Introduction and Background 1
2. Hydrogen Evolution System 4
3. Phycobilisome-containing Organisms 4
    - *a. Synechocystis* PCC 6803 5
    - *b. Thermosynechococcus elongatus* BP-1 5
    - *c. Chroococcidiopsis* TS-821 5
    - *d. Synechococcus* WH 7803 6
    - *e. Synechococcus* WH 8102 6
4. Phycobilisome Intracellular Location 7
5. General Structure of the Phycobilisome Complex 7
6. Phycobilisome Chromophores 12
7. Linker Proteins 14
8. The Allophycocyanin Core 17
9. The Phycobilisome Rods 19
    - a. Phycocyanin 19
        - i. C-PC/R-PC 20
        - ii. PC_{620}/PC_{612} 20
        - iii. PC_C (PC1)/PC_I(PC2) 21
    - b. Phycoerythrin (PE_I and PE_{II}) 21
    - c. FNR_L attachment 22
10. CpcG1 and CpcG2 23
11. State Transitions 23
12. Chromatic Adaptation 24
13. Specific Interactions with PSI and PSII 25

Chapter 2: Design of a PSI-CpcG2 Fusion **28**

1. Introduction 28
2. PSI Subunits 28
    - a. PsaK 30
    - b. PsaX 33
    - c. PSI Subunit Analysis 33
3. CpcG2: Additional Background and Analysis 34
4. Fusion Design 39
5. Location for HindIII Restriction Site and Kanamycin Resistance Drop-in 43
6. Statement of Research Goals 44

Chapter 3: Methods and Materials **45**

1. PCR 45
2. Transformation and Plasmid Isolation 45
3. Cell Culturing 46
4. Purification of Phycobilisomes 46
5. Tricine-SDS-PAGE 48

6. Absorbance Measurements 48
7. Steady-State Fluorescence 49
8. Stopped-Flow Fluorescence 49
9. Chaotrope Dissociation Assay 50
10. pH Assay 50

Chapter 4: Results **52**
1. Progress in CpcG2-PSI Fusion 52
2. Phycobilisomes Isolation 55
3. Dissociation of Phycobilisomes 59
    a. Chaotropic Dissociation of Phycobilisomes 59
    b. Low Phosphate Dissociation of Phycobilisomes 63
    c. pH Dissociation of Phycobilisomes 67

Chapter 5: Discussion and Conclusion **72**
1. CpcG2-PSI Fusion 72
2. Phycobilisomes Dissociation 73
3. Conclusion and Future Directions 79

Bibliography **80**
Appendices **89**
Vita **98**

Table of Figures

1.1 Absorption Spectra for Phycobilisomes and PSI 3
1.2 Model of Phycobilisome Hexamer Assembly 8
1.3 Phycobilisomes Hexamer Structural Measurements 9
1.4 Representative 2D Image of A Phycobilisome Complex 11
1.5 Prosthetic Bilin Chromophores found in Phycobilisomes 13
1.6 Schematic View of an APC Core 18
1.7 Methods for Phycobilisome Interaction with PSI and PSII in the Membrane 27

2.1 Design Scheme for the *In Vitro* Association of Phycobilisomes to Photosystem I 29
2.2 PsaX and PsaK in Photosystem I 31
2.3 Projected Spacial Distribution of Phycobilisomes Attached to CpcG2-PSI Fusions 32
2.4 CpcG1 Protein Sequence Alignment 35
2.5 CpcG2 Protein Sequence Alignment 36
2.6 Hydropathy Plots for CpcG1 and CpcG2 38
2.7 Molecular Biology Plan for Creating the CpcG2-PSI fusion 40

4.1 Agarose Gel of the CpcG2 Linker with Ser-Ser-Thr Spacer Sequences 53
4.2 Modified PsaX Digested with RsrII and HindIII 54
4.3 Purification of Phycobilisomes on a Sucrose Density Gradient 56
4.4 Tris-Tricine Gel Electrophoresis of Blue Phycobilisomes 57
4.5 Tris-Tricine Gel Electrophoresis of Phycobilisomes Isolated from *Synechococcus* WH 7803 and *Synechococcus* WH 8102 58
4.6 Chaotropic Dissociation of Phycobilisomes in the presence of NaCl 61
4.7 Chaotropic Dissociation of Phycobilisomes in the presence of Urea 62
4.8 Low Phosphate Dissociation Kinetics of Phycobilisomes Isolated from *Synechocystis* PCC 6803 65
4.9 Low Phosphate Dissociation Kinetics of Phycobilisomes Isolated from *Synechococcus* WH 8102 66
4.10 pH-Dependent Dissociation of Blue Phycobilisomes 69
4.11 pH-Dependent Dissociation of Phycobilisomes Isolated from *Synechococcus* WH 8102 70

5.1 Mutation of RsrII Restriction Site 72

List of Abbreviations

PBSome	phycobilisome
PB	phycobilin
PBP	phycobiliprotein
APC	allophycocyanin
PC	phycocyanin
PE	phycoerythrin
PCB	phycocyanobilin
PEB	phycoerythrobilin
PUB	phycouribilin
PSI	photosystem I
PSII	photosystem II
L_R	rod linker
L_{RC}	rod-core linker
L_C	core linker
L_{CM}	core-membrane linker

Chapter 1: Phycobilisomes

1. Introduction and Background

The driving force behind the search for alternative energy sources not based on fossil fuels has been accelerated recently by the rising concern for increasing costs of energy, the undesirable prospect of hitting a peak in oil production, and the hope of attaining energy security for the country and the future (Pimentel 1991; Lloyd and Subbarao 2009). Biologically-derived fuels, or biofuels, are one of several targets for alternative energy pursuits because of its potential for sustainability. As such, research into biofuel production has seen an increase in funding over the past few years, with much attention given to the fact that biofuels could be carbon neutral (Hossain, Salleh et al. 2008), if not carbon sequestering (Tilman, Hill et al. 2006). A common thread in biofuel production is the dependence on photosynthesis, nature's method for converting of light energy into chemical energy. Photosynthesis can be utilized in the formation of hydrogen, which can then serve as a convenient and renewable biofuel (Das and Veziroğlu 2001). Purified photosynthetic proteins are reported to be capable of producing hydrogen that is the equivalent to 300 liters of gasoline per hectare per day (Iwuchukwu, Vaughn et al. 2009). Manipulating the photosynthetic machinery could potentially be a powerful tool for the production of hydrogen as an alternative energy source, but, as with most new technologies, improvements in the efficiency of hydrogen production can be made.

Photosystem I (PSI) is the primary photosynthetic component in the evolution of hydrogen, and is responsible for both the capture and utilization of

ambient light to produce hydrogen molecules. Multiple chlorophyll pigments bound to PSI confer it the ability to absorb light, but only at a limited portion of the electromagnetic spectrum (Figure 1.1) (Brown 1983). Improving the absorption efficiency of this system is one way to increase hydrogen production. The latter can be accomplished by another protein complex found within cyanobacterial species called the phycobilisome (PBSome). The goal of this study is to investigate the chemical and physical properties of PBSomes in an effort to incorporate these complexes into the existing hydrogen evolution system and increase its efficiency.

PBSomes are macromolecular complexes found in a variety of photosynthetic organisms, including cyanobacteria, which function in capturing light and subsequently delivering that energy to the reaction centers of PSI and photosystem II (PSII) (Mullineaux 2007). These light harvesting antennae may be produced in large amounts, accounting for 50% of the soluble protein within a cell (Grossman, Schaefer et al. 1993). In contrast to the chlorophyll chromophores of PSI and PSII, the PBSome complexes may use a variety of different bilin chromophores as their means of capturing light. The number of chromophores can range from a few hundred to over a thousand chromophores per PBSome complex (Gantt 1996; Parbel and Scheer 2000). Also, unlike other accessory light-harvesting structures, PBSomes are largely hydrophilic and not integral membrane proteins (Glazer 1984). The light-absorbing properties of PBSomes enable it to utilize a larger portion of the visible spectrum than would otherwise be possible by PSI and/or PSII alone (Figure 1.1) (Sidler 1994).

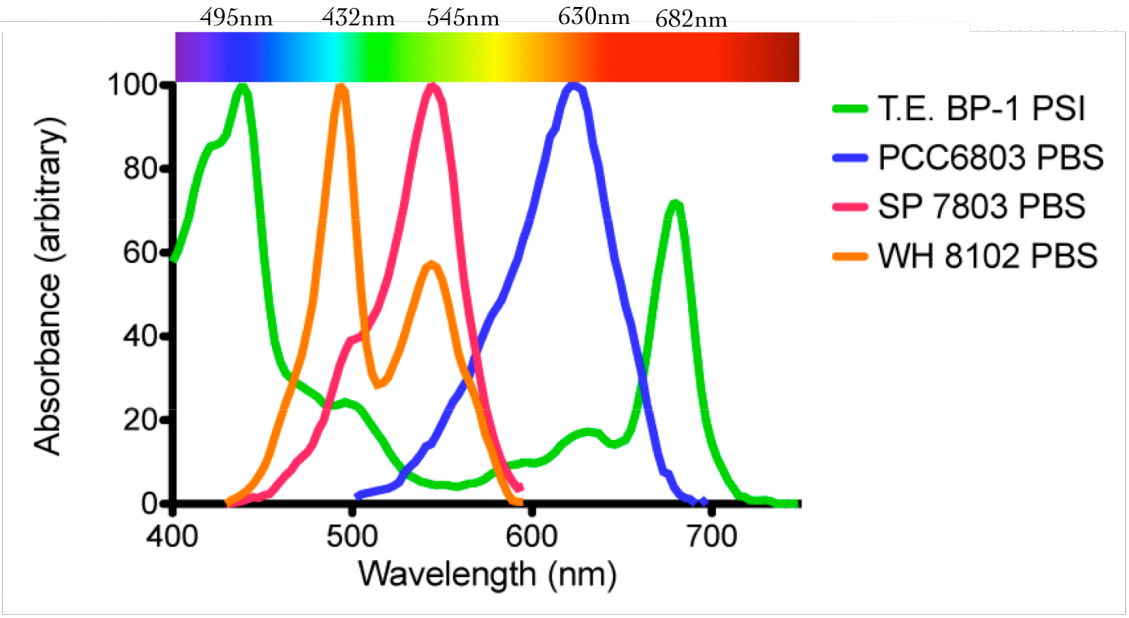


Figure 1.1. Absorbance Spectra for Phycobilisomes and PSI. Relative absorbances of PBSomes isolated from *Thermosynechococcus elongatus* BP-1 (green), *Synechocystis* PCC 6803 (blue), *Synechococcus* WH 7803 (red), and *Synechococcus* WH 8102 (orange) is plotted against wavelength. PBSome absorbance is the greatest in the visible spectrum where chlorophyll absorption is the least efficient.

2. Hydrogen Evolution System

The current design for hydrogen evolution involves a combination of PSI isolated from *Thermosynechococcus elongatus*, ascorbate as an artificial electron donor, and cytochrome c as an intermediate electron donor (Iwuchukwu, Vaughn et al. 2009). PSI is capable of absorbing light at its reaction center, named P700, and using the captured energy to excite an electron to a higher energy level for an energetically uphill electron transfer. When platinized to create a catalytic surface, PSI can donate this excited electron to platinum (Pt) to facilitate hydrogen evolution. To continue this process, PSI must be returned to its reduced ground state. The latter occurs by oxidation of ascorbate, resulting in the reduction of cytochrome c, which subsequently delivers its electron to PSI. Thereby, hydrogen evolution by this system requires light energy, but PSI is the only light-capturing protein present with its collection of chlorophylls, which provides limited light absorption capabilities. By including PBSomes in this system, additional light may be captured and utilized for H_2 production.

3. Phycobilisome-containing Organisms

Five organisms are used in this study. The diversity of the organisms allowed for comparisons between organisms from differing environments. The environments these organisms live in include mesophilic freshwater and saltwater environments, as well as freshwater thermophilic habitats. The PBSomes from these five organisms display three distinct light absorption profiles due to differences in the chromophores and chromophore ratios employed, and are described below.

3.a. *Synechocystis* PCC 6803

Synechocystis PCC 6803 is a photosynthetic cyanobacterium first discovered in 1968 in a freshwater lake in California. This organism can live in the dark, but requires a short duration (5-15 minutes) of light a day to survive, even with PSI and PSII deletions (Anderson and McIntosh 1991). PBSomes isolated from this organism contains only phycocyanobilin (PCB) chromophores. The *Synechocystis* PCC 6803 genome is sequenced, and the species is readily transformable (Chauvat, Vries et al. 1986; Xu, Vavilin et al. 2004).

3.b. *Thermosynechococcus elongatus* BP-1

Thermosynechococcus elongatus BP-1 is a freshwater thermophilic cyanobacterium found in the Beppu hot springs in Japan. PSI has been successfully isolated and crystallized from this organism, and also employed in various hydrogen evolution studies (Schubert, Klukas et al. 1997; Jordan, Fromme et al. 2001). PBSomes isolated from this organism are blue in color and contain only PCB chromophores. The genome of *T. elongatus* BP-1 is sequenced, and the species can be amenable to transformation.

3.c. *Chroococcidiopsis* TS-821

Chroococcidiopsis TS-821 is another thermophilic cyanobacterium, and was discovered in a hot spring in Thailand. *Chroococcidiopsis* TS-821 is capable of growing at 50°C with CO_2 concentrations as high as 10%. This organism is reported to secrete sugars into the nearby environment to a concentration as high as 1 mg/ml (Ishida, Hasegawa et al. 1997). The PBSomes isolated from

Chroococcidiopsis TS-821 are blue in color and contain only the PCB chromophore.

3.d. *Synechococcus* WH 7803

Synechococcus WH 7803 is one of the first phycoerythrobilin (PEB)-containing cyanobacteria to be cultured axenically and studied (Morris and Glover 1981). In 1978, this cyanobacterium was discovered at a depth of 25 meters below the surface of the Sargasso Sea (Campbell and Iturriaga 1988), a body of water rich in nutrient salts. *Synechococcus* WH 7803 is a mesophilic organism whose genome has been sequenced, and can be readily transformed via conjugation (Brahamsha 1996). The PBSomes produced by this organism are red in color and contain PCB, PEB, and phycourobilin (PUB) chromophores. The PUB:PEB ratio seen in *Synechococcus* WH7803 PBSomes is 0.44 ± 0.004 (Six, Thomas et al. 2007)

3.e. *Synechococcus* WH 8102

Synechococcus WH 8102 is another marine cyanobacterial species and was discovered in the Sargasso Sea in 1981. Like *Synechococcus* WH 7803, *Synechococcus* WH 8102 is also an obligate marine organism that grows at mesophilic temperatures. The PBSomes within this organism are purple in color and contain PCB, PEB, and PUB chromophores. The PUB:PEB ratio is over four times greater than that present in *Synechococcus* WH 7803, at 1.88 ± 0.122 (Six, Thomas et al. 2007).

4. Phycobilisome Intracellular Location

Within the chloroplast, which is the subcellular organelle that serves as the site of photosynthesis, the PBSome complex is located in the cytosolic space between the layered thylakoid membrane and the chloroplast membrane called the stroma. In order to be useful to the photosynthetic process, PBSomes must remain close to the photosynthetic apparatus to ensure rapid acclimation to changing light conditions (Yang, Zhang et al. 2009). Presently, direct evidence to suggest that any part of the PBSome complex is physically connected to the thylakoid membrane does not exist.

5. General Structure of the Phycobilisome Complex

The structural format of PBSomes is well-conserved across species; however, the exact structure-chromophore composition of PBSomes can differ dramatically, resulting in a wide variety of colors in the containing organisms (Six, Thomas et al. 2007). The general structure of the PBSome complex is a cylindrical **core** surrounded by six cylindrical **rods** extending from the core. The basic building block of each core and rod of this complex is the alpha-beta (αβ) monomer (Figure 1.2). The use of 'α' and 'β' is the generic nomenclature for the two pieces that comprise the majority of the PBSome structure, but may or may not refer to the same gene products. For instance, the α and β units of the PBSome rods are products of different genes from that of the α and β subunits of the core. Each αβ monomer may contain between two to five bilin chromophores depending on its location in the PBSome complex, with distal rod cylinders containing a greater number of chromophores. Three identical αβ monomers

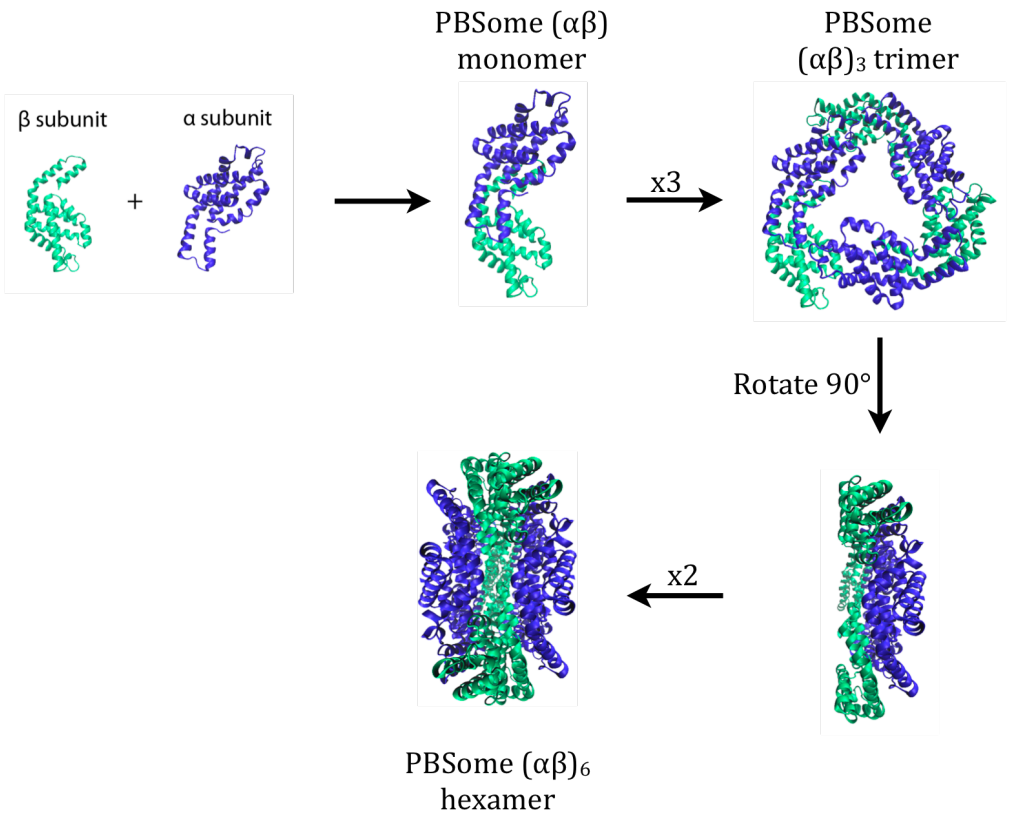


Fig 1.2: Model of Phycobilisome Hexamer Assembly. An α and β subunit combine to form a PBSome monomer. This monomer is formed after the bilins have been attached. Three monomers associate form a trimer structure with an outer diameter of roughly 12 nm and an inner diameter of about 3 nm. Two trimers associate via the β surfaces facing each other to form a hexameric subunit (adapted from Adir, 2006).

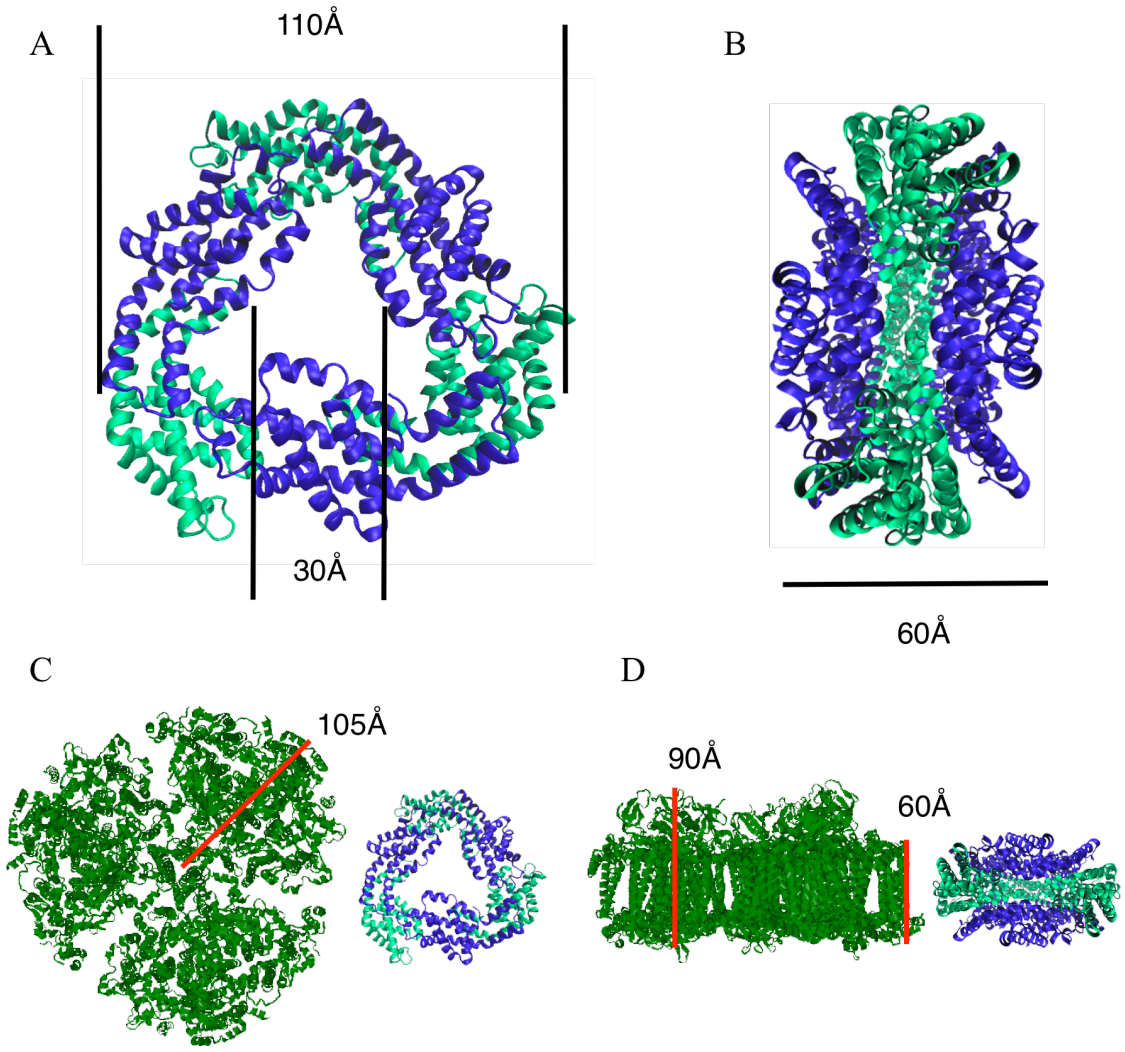


Figure 1.3: Phycobilisome Hexamer Structural Measurements. (A) Inner and outer diameters of each PBSome hexamer measure 30Å and 110Å, respectively. (B) The width of the hexamer is 60Å. For comparison, (C) PSI (*left*) has a radius of 105Å from its center to the residue furthest from this point, and (D) its height is 60Å and 90Å from the lumenal to stromal surface and lumenal to highest point of the stromal hump of PSI, respectively. [PSI PDB ID:1JB0, Jordan P. *et al.* (2001), *Nature*, 411:909-917; PBSome PDB ID: 1B33, Reuter W. *et al.* (1999), *Proc. Natl. Acad. Sci.USA,* 96: 1363-1368]

can assemble to form a trimer, designated $(\alpha\beta)_3$, which is arranged in a circle with an outer diameter of nearly 110Å and an inner diameter of roughly 30Å, creating a central void (Figure 1.3). The α components of the trimer face one side of the circle, while the β components face the other side. Two matching $(\alpha\beta)_3$ trimers can subsequently combine to form a $(\alpha\beta)_6$ hexamer in the shape of a disk, with the α units of the trimers at the interface in the hexamer. These hexameric disks are then stacked into cylinders to form the individual core and rod units of PBSome complex (Bryant, Guglielmi et al. 1979).

The typical PBSome possesses a central allophycocyanin (APC) core composed of the cylinders generated from $(\alpha\beta)_6$ hexameric disks, which are stacked in parallel (Figure 1.4A). Branching off of the APC core are six rods, also composed of multiple, stacked cylinders. Two types of rods are primarily found in PBSomes, phycocyanin (PC) and phycoerythrin (PE). These rods serve as the primary site of light capture and subsequently deliver the light energy captured to the APC core in a unidirectional manner towards its final destination at a photosystem reaction center (Liu, Chen et al. 2010).

The discovery of colorless linker proteins (Figure 1.4B), responsible for facilitating and maintaining the assembly of hexamers into larger cylinders, occurred years after research began on PBSomes (Tandeau de Marsac and Cohen-Bazire 1977). Roughly 15% of the PBSome mass is due to the linkers included in the complex. All together, the mass of a PBSome may range between 2 to 15 megadaltons depending on the organism and its growth conditions (Mullineaux 2007). Linker proteins are generally found in the central

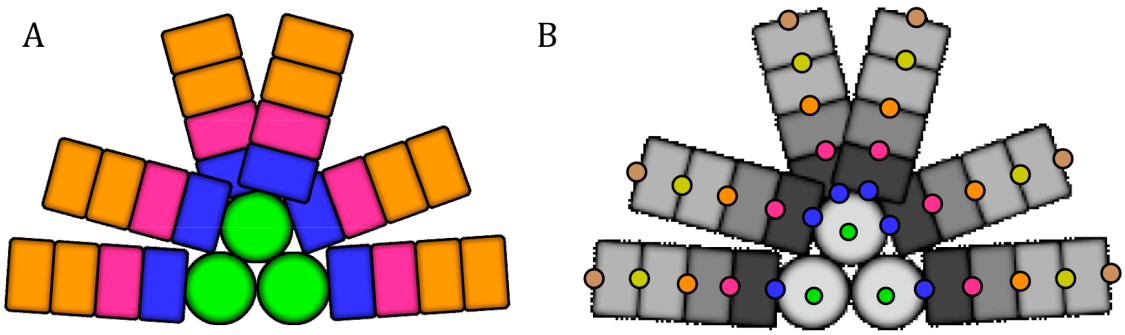


Figure 1.4: Representative 2D Image of A Phycobilisome Complex. (A) The hypothetical PBSome complex is commonly depicted with a tri-cylindrical APC core and six rods radiating outward (Adir, Dines et al. 2006). The rods consist of a phycocyanin base (blue) with a phycoerythrin I (magenta) and two phycoerythrin II (orange) hexamers attached. (B) Linker peptides are organized inside the multimeric superstructure to hold the complex together. From the center radiating outwards are core L_C linkers (green), L_{RC} rod-core linkers (blue), a system of L_R rod linkers (pink, orange, yellow), and linker-like cap peptides (brown). Partitioned subunits in this model represent hexameric subunits.

channel formed by the 30Å void space at the center of a hexamer.

6. Phycobilisome Chromophores

The brilliant and varied colors of PBSomes are attributed to the bilin chromophores covalently bound to the complex. Covalent binding of the chromophore to the apoprotein provides photometric activity, structural stability, and absorbance optimization of the phycobiliprotein's (PBP) monomeric constituents (Toole, Plank et al. 1998). The multiple bilins that can be used by PBSomes are derived from the same precursor, biliverdin (BV), through a sequence of chemical reactions involving ferredoxin-dependent bilin reductases and isomerases (Figure 1.5) (Scheer and Zhao 2008). BV has a linear tetra-pyrrolic structure and is green in color. Alternative bilin chromophores, such as phycocyanobilin (PCB), phycoerythrobilin (PEB), and phycouribilin (PUB), arise from the modification of the first and/or fourth pyrrole of BV, resulting in blue, red, and orange pigments in PBPs, respectively. These modifications to BV include three distinct reductions and at least one isomerization reaction, but only a combination of up to two at a time can take place (Scheer and Zhao 2008). Binding to the apoprotein also takes place at the first and/or fourth pyrrole, but only if there is a free vinyl group available to bind to the conserved cysteine residues of the α or β subunits of the PBSome.

PCB is produced by the reduction of C2-C3 double bond of the first pyrrole ring and the vinyl group of the fourth pyrrole of BV (Figure 1.5). Both reductions are catalyzed by the reductase PcyA (Frankenberg and Lagarias 2003). The

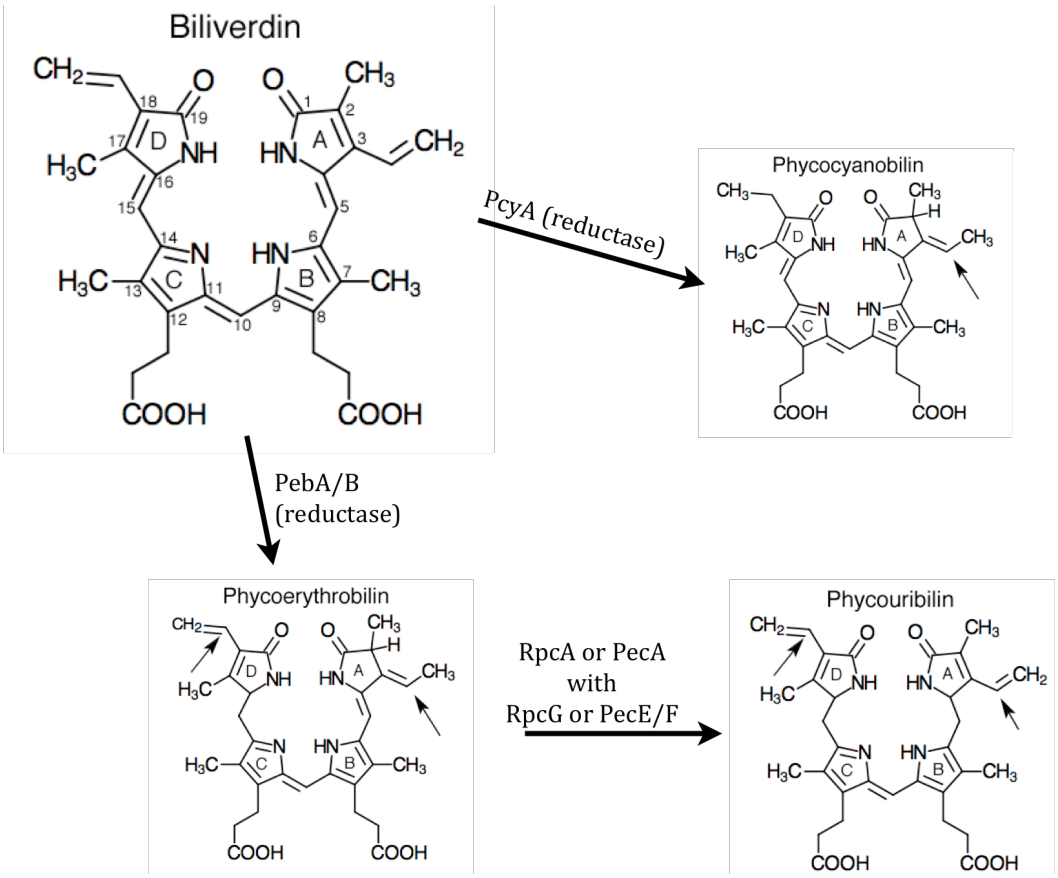


Figure 1.5: Prosthetic Bilin Chromophores found in Phycobilsiomes. Biliverdin is the precursor from which all others chromophores are derived. *T. elongatus* BP-1, *Synechocystis* sp. PCC 6803, and *Chroococcidiopsis* sp. strain TS-821 produce only phycocyanobilin (PCB). *Synechococcus* sp. WH7803 produces both PCB and phycoerythrobilin (PEB), while *Synechococcus* sp. WH8102 produces PCB, PEB and phycouribilin (PUB). Other bilins, such as phytochromobilin found in plants (Kohchi, Mukougawa et al. 2001) and mesobiliverdin utilized by cryptophytes, are derived from biliverdin through additional reactions.

apoprotein binds the PCB chromophore through the unmodified vinyl group of the first pyrrole via a conserved cysteine residue. PEB differs from PCB at the fourth pyrrole, where reduction occurs at the C15-C16 double bond, leaving the vinyl group on C18 free for possible binding to the apoprotein. Reduction of BV into PEB is achieved by either a two-step method, involving the reductases PebA and PebB with a 15/16 dihydrobiliverdin intermediate, or through a single enzyme, PebS. Lastly, PUB is derived from a PEB precursor that is modified via isomerization at the first pyrrole.

The BV-derived chromophores described have distinct spectral properties (Figure 1.1). The PCB, PEB, and PUB chromophores have an absorption maximum at 631 nm, 545 nm, and 495 nm, respectively. Upon light absorption, if a chromophore in its excited state fails to transfer its resonance energy to a neighboring chromophore, fluorescence occurs. PCB has a fluorescence emission maximum at 677 nm when bound at the ACP core and at 650 nm in the PC rods, while PEB has a single emission at 563 nm. Unlike the latter, PUB is not known to fluoresce in PBSomes.

7. Linker Proteins

To maintain the overall structure of the PBSome complex, linker proteins are employed to stabilize the interactions between hexamer sub-complexes (cf. Appendix 1 and Fig. 1.4B). This family of proteins is divided into four groups based on location in the complex. Rod linkers (L_R) are located in the rod structure connecting PEB- and PCB-containing subunits. The L_R subgroup of linkers also includes γ linkers. Rod-core linkers (L_{RC}) are found between the first

hexamer at the base of the rod and the APC core to which the rod attaches. Core linkers (L_C) are involved in maintaining the base APC core complex, and have been shown to be essential to APC core stability (Ajlani, Vernotte et al. 1995). Upon its deletion, PBSomes fail to assemble into mature complexes (Ajlani, Vernotte et al. 1995). In addition to the latter three linkers, the core-membrane linker (L_{CM}) proteins attach the APC core to the thylakoid membrane, but its exact mechanism of function is still unknown. Linker proteins are specific their purpose and location, and except for the L_{CM} and γ linkers, lack bilin chromophores. Linker protein are also present at a near 1:1 ratio with $(\alpha\beta)_6$ hexamers of the PBSome (David, Marx et al. 2011).

L_R proteins are buried within the PBSome rods structure and maintain hexamer-hexamer interactions. TEM studies of PBSome complexes fail to visualize the L_R linker proteins, indicating that these proteins are buried within the complex. L_R linkers interact with each other through the 30Å void that runs through the rod hexamers (Figure 1.3) (Liu, Chen et al. 2005). The interaction of these linkers at the central channel of hexamers enables it for the coordination of organized rod assembly without the risk of repeating hexamers unnecessarily.

Crystallographic data of linkers is limited to the L_C linker, where it was successfully crystallized within a single $(\alpha\beta)_3$ trimer (Reuter, Wiegand et al. 1999). This structure shows that the L_C interacts with two of the three β subunits in an APC trimer. The latter, however, may not correlate to interactions of other linkers within the PBSome, including the L_R linkers found in the rods, which have been shown to interact with each other through the central void space of the $(\alpha\beta)_6$

hexamers (Liu, Chen et al. 2005). Linker-linker interactions are unnecessary for core L_C linkers, as L_C linkers maintain APC hexamer stability, while L_R linkers maintain and stabilize the interaction between hexamers in the rod cylinders.

The L_{CM} is the largest of the linker proteins, with a mass typically around 130 kDa. In contrast to other linkers found in the void space, the L_{CM} replaces one of the α subunits in a $(\alpha\beta)_3$ trimer (Adir 2005). Depending on the organism, the L_{CM} protein can be divided into two or more functional parts (MacColl 1998). In general, the N-terminal domain resembles the α subunit it replaces in an APC monomer and the C-terminal region is believed to be involved in the interaction with membrane. Although the L_{CM} does not enter the membrane, as it has no transmembrane domains (Capuano, Braux et al. 1991), the mechanism by which the L_{CM} interacts with the thylakoid membrane is still under investigation.

Interactions between linkers and their respective PBPs are strong and via a combination of hydrophobic and electrostatic interactions (Zilinskas and Glick 1981). The former hydrophobic interactions are entropically-driven by interrupting the structured ordering of surrounding water molecules. Studies in varying the ionic strength of different buffers on PBSome stability revealed that phosphate particularly stabilizes these complexes, likely by interacting with the surrounding water molecules and interfering with its hydrogen bonding in these complexes (Hatefi and Hanstein 1974). The latter electrostatic interaction can be inferred from the general basic nature and high pI of linkers, and the relatively acidic and low pI of the PBPs to which they bind (Adir, Dines et al. 2006). Upon integrating into the PBSome complex, the linkers may modify nearby

chromophores and affect their absorption or fluorescence (MacColl 1998; Pizarro and Sauer 2001). By modifying the spectral characteristics of nearby chromophores, the linkers can reinforce the unidirectional pathway for energy transfer within the PBSome (Grossman, Schaefer et al. 1993).

8. The Allophycocyanin Core

Allophycocyanin (APC) is the central core of the PBSome complex (Figure 1.4), and is the final site of exciton activity before the complex either donates the energy to the reaction center of PSI/PSII or fluoresces. APC cores containing two, three, or five parallel cylinders are known to exist (Kondo, Geng et al. 2005). In the organisms discussed in this work, the APC core is composed of three cylinders organized in a triangle shape with their lengths appearing to run parallel to each other (Figure 1.6). The base of the three-component APC core is composed of two APC cylinders anti-parallel to one another. Each of these two cylinder is composed of four APC $(\alpha\beta)_3$ trimer rings [or two $(\alpha\beta)_6$ hexamers]. The trimer rings, however, are not identical. The first and second $(\alpha\beta)_3$ trimers are products of the *apc*A and *apc*B genes and are bound together by an L_C linker. The third $(\alpha\beta)_3$ trimer contains two substitutions, where a single α subunit is replaced with the N-terminal domain of the L_{CM} linker (*apc*E) and a β subunit is replaced with the *apc*F gene product, named β^{18} (MacColl 2004). The final $(\alpha\beta)_3$ trimer in the series has a single change, where a single α component is replaced by an alternative α subunit translated from gene *apc*D. In contrast to these base cylinders, the third apex cylinder of the APC core is comprised two $(\alpha\beta)_6$ hexamers with unmodified $(\alpha\beta)_3$ trimers and a single L_C linker between the first

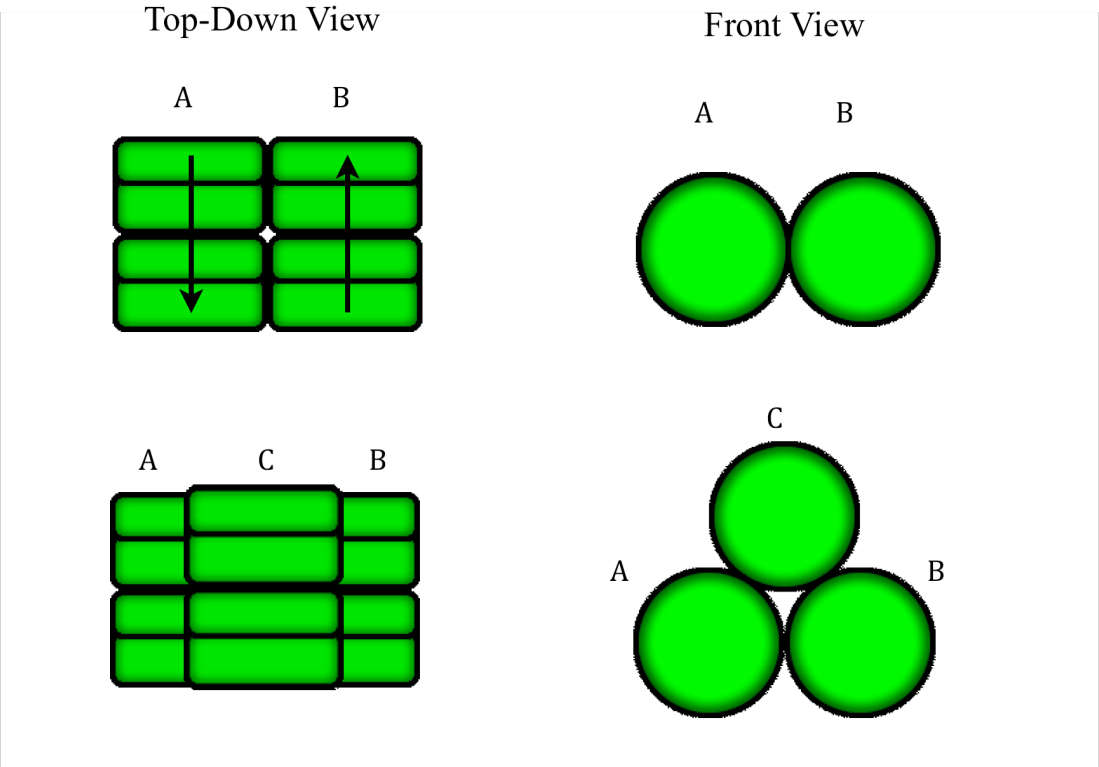


Figure 1.6: Schematic View of an APC Core. The top left view shows the antiparallel direction of the base APC cylinders (A and B), as indicated by the arrows. The four individual trimer subunits per cylinder each have distinct and identifiable substitution. The bottom left diagram shows a third apex cylinder (C) sitting atop the base cylinders. This cylinder has no directionality, as all trimer subunits are identical. The front views on the right are presented to help visualize the cylinders spacial location within the PBSome.

and second pair of $(\alpha\beta)_3$ trimers (Gingrich, Lundell et al. 1983). Each α and β subunit of the APC (and their potential substitutes) binds a single PCB chromophore at a conserved cysteine residue at or around position 82, or Cys195 for L_{CM}.

While the precise function of each subunit in the APC structure is still being elucidated, various deletion mutants of the subunits were made in *Synechocystis* sp. PCC 6803 and *Synechococcus* 7002 to try and understand functions of the different subunits. Disruption of *apc*F or *apc*D had no noticeable effect on PBSome spectral properties in either of the studied species (Ashby and Mullineaux 1999; Dong, Tang et al. 2009). In *Synechocystis* PCC 6803, *apc*AB^-, as well as *apc*E^-, strains fail to produce functional PBSomes (Ajlani, Vernotte et al. 1995), indicating their necessity for assembly of the APC core.

9. The Phycobilisome Rods

The PBSome rod is the site where the majority of light capture occurs, which is the reason their incorporation into the current hydrogen evolution system is desired. Most of the PBSome chromophores can be found in the rods. Like the APC core, the rod is an assembly of (αβ) monomers arranged into hexamers. The hexamers are stacked together to form rod structures with the help of L_R rod linkers. The first hexamer of the rod is the phycocyanin (PC), followed either by additional PC or phycoerythrin (PE) hexamers.

9.a. Phycocyanin

PC is the terminal pigmented energy acceptor in the PBSome rod sub-

complex, and is present in all PBSomes. The physical conformation of the PC is analogous to the APC and the rest of the PBSome complex; however, there are three classifications of PC to be addressed: C-PC/R-PC, PC_{620}/PC_{612}, & PC_C/PC_I (also referred to as PC1/PC2, respectively).

9.a.i. C-PC and R-PC

C-PC is a form of PC that binds only PCB chromophores. In fresh-water cyanobacteria, the C-PC may constitute the entire rod (Sidler 1994). In contrast, R-PC is a PC subunit that binds both PCB and PEB chromophores. This type of PC is commonly found in PE-containing cyanobacteria.

9.a.ii. PC_{620} and PC_{612}

PC_{620} is the primary form of PC and the primary constituent of the rod structure of blue-green algae and cyanobacteria. The pigment found within the PC is PCB, which imparts an absorbance peak maximum near 620 nm for this complex (Olive, Ajlani et al. 1997). The structure of the PC_{620} subunit is an $(\alpha\beta)_6$ hexamer composed of two $(\alpha\beta)_3$ trimer discs, one rotated 180° in relation to its partnered trimer (Padyana, Bhat et al. 2001). Each monomer binds three PCB chromophores, one each at αCys84, βCys84 and βCys155, which are residues conserved across species. In the hexameric $(\alpha\beta)_6$ form, the PCB at β155 is located outside the ring and exposed to the solvent, and thus, possibly the responsible cofactor for energy propagation down the PC rod to the APC core (Stec, Troxler et al. 1999).

PC_{612} is a unique PC structure, currently only documented in

Thermosynechococcus vulcanus, and is located at the base of the PBSome rods where it associates with the APC (David, Marx et al. 2011). Unlike PC_{620}, PC_{612} exists as a $(\alpha\beta)_3$ trimer; its blue-shifted absorbance at 612 nm is caused by a lack of methylation at βAsn72 (Adir 2003), whereas methylation of this residue would result in the red-shifted absorbance observed by the PCB bound-PC to the βCys84 residue. The trimeric conformation of this PC subunit allows it flexibility, possibly allowing for better connectivity with the curved sides of the APC core (Adir, Dines et al. 2006).

9.a.iii. PC_c and PC_l (also referred to as PC1 and PC2, respectively)

This classification is reserved for chromatically-adaptive cyanobacteria, which are capable of modulating the chromophores it synthesizes to adjust to changing light conditions. The PC_c is the constitutive PC present in all PBSome rod complexes in these organisms (Hirose, Shimada et al. 2008). These PC_c are situated proximally to the APC core. PC_l is the inducible form of PC that may be added to the PC_c to extend the rod length and increase the light capturing capabilities of the organism (Hirose, Shimada et al. 2008). PC_l is expressed experimentally under red light conditions (Grossman, Schaefer et al. 1993); otherwise, this rod subunit may be preferentially replaced with PE.

9.b. Phycoerythrin

PE is only present in certain cyanobacteria and red algae, and is located at the distal end of the PBSome rod when present. The pigmentation found in the PE subunit can vary widely among species and environmental conditions (Six, Thomas et al. 2005). The result is a change in spectral properties, which can be

attributed to inclusion of a combination of PEB and PUB chromophores. PE is divided into two categories, PEI and PEII, depending on the chromophores bound. PEII binds a combination of both PEB and PUB chromophores, while PEI may bind either both chromophores or only PEB (Ong and Glazer 1991). The sites for bilin attachment to cysteine residues are conserved at positions α84, β84, and β155, but additional cysteines with chromophores bound at α143, β50 and β61 can also be found. PE is assembled into $(\alpha\beta)_6$ hexamers, but with the addition of a bound γ linker (*Mpe*C) subunit. A unique feature of this γ linker is its ability to bind up to four chromophores (Scheer and Zhao 2008).

9.c. FNR_L Attachment

At the distal end of a PBSome rod, either a rod-capping L_R linker protein or a ferredoxin:$NADP^+$ oxido-reductase (FNR) enzyme with a rod linker-like domain is present. Ferredoxin (Fd) is the final electron carrier in the electron transport pathway in photosynthetic organisms. This carrier delivers electrons to FNR, which is responsible for reduction of $NADP^+$ to NADPH. Limited studies on FNR attachment to PBSomes are available (Korn, Ajlani et al. 2009). Some organisms have two forms of this enzyme: large (FNR_L) and small (FNR_S). The additional N-terminal residues of FNR_L resemble the N-terminus of L_R proteins in PBSome rods, which allows FNR_L to bind to the distal $(\alpha\beta)_6$ hexamer of a PBSome rod (Adir, Dines et al. 2006). Evidence for energy transfer between the FNR_L and the PBSome complex does not exist.

In addition to the structural difference, the activity of the two FNRs differs slightly. FNR_L has been shown to be a better reductase, while FNR_S acts as a

better oxidase (Korn, Ajlani et al. 2009). By inference, FNR_L is bound to PBSomes to keep it localized in the thylakoid and easily accessible for reductase activity at the membrane. The latter arrangement would also prevent FNR_L from diffusing into the cytoplasm and interfering with respiration.

10. CpcG1 and CpcG2

The L_{RC} linker is responsible for maintaining the connection between the base PC subunit of the rod and the APC core. L_{RC} is a generic name for the CpcG1 protein. Sequencing of the *Synechocystis* PCC 6803 genome revealed the existence of a second CpcG gene, named CpcG2 (Takakazu, Sato et al. 1996). Further sequencing results have shown that *Synechocystis* PCC 6803 is not unique in having two forms of the CpcG linker (Kondo, Geng et al. 2005). The CpcG family can be divided into these two groups based on amino acid sequence and character of its C-terminal residues. The C-terminal residues of CpcG1 are hydrophilic, whereas CpcG2 contains a hydrophobic C-terminus, which is predicted to be a transmembrane domain (Kondo, Ochiai et al. 2007).

In addition to C-terminal composition, the two CpcG forms differ to which it connects the PBSome rod. CpcG1 links the PBSome rods to the APC core. CpcG2 can be used in its stead, but will not lead to the association of the rod to the core; the hydrophobic C-terminal domain of CpcG2 leads to its tight association with the thylakoid membrane (Kondo, Ochiai et al. 2007).

11. State Transitions

Since light conditions are not constant in nature, changes in light quality

and quantity must be continuously accounted. Under high light conditions, if light is captured at a rate greater than it can be consumed, damage of the cell by the formation of reactive oxygen species may occur (Asada 1994). One method by which a photosynthetic organism may compensate for changing light conditions is by state transitions. Two state transitions exist and are named according to the reaction center that is optimally saturated with light. A state I transition occurs when PSI activity is optimal, leading to the movement of PBSomes to transfer energy to PSII. Likewise, state II transitions function in the reverse role to transfer energy from PBSomes to PSI when PSII is optimally active (Kondo, Geng et al. 2005). Cyanobacteria use state transitions as a mechanism for regulating the photosynthetic electron transport pathway, and balancing PSI and PSII to work together efficiently under varying light conditions (Haldrup, Jensen et al. 2001; Wollman 2001; Allen 2003; Walters 2005).

12. Chromatic Adaptation

In contrast to state transitions, complimentary chromatic adaptation (CCA) is an alternative way that some organisms can adjust to changing light quality (Kehoe and Gutu 2006). Where state transitions modulate the efficient use of captured light energy and optimize PSI/PSII activity, CCA moderates the efficient capture of light in changing light quality. CCA is divided into four types, based on the mechanism of adaptation. While many photosynthetic organisms do not undergo any form of chromatic adaptation, type II and type III adaptation are the forms most widely seen in cyanobacteria. Type II is characterized by changes in PE production without any change to the production of the PC subunit

(Anderson, Rayner et al. 1984). Type III chromatic adaption regulates synthesis of both PC (involving PC1 and PC2) and PE (Conley, Lemaux et al. 1988). Type IV chromatic adaption is mechanistically different in that it does not change the transcription of phycobilisome subunits. Instead, the change is in the chromophorylation of the PEI and PEII subunits (Everroad, Six et al. 2006).

13. Specific Interactions with PSI and PSII

Although the exact mechanism by which the PBSome interacts with reaction centers has not been solved, the PBSome complex can deliver light energy to PSI and PSII in a controlled, deliberate manner (Mullineaux 2007). Several hypotheses by which the PBSome interacts with and transfers energy to the reaction centers have been proposed (Biggins 1985; Mullineaux 1992), as displayed in Figure 1.7. In the most common mechanism (Figure 1.7A), the PBSome associates with the PSII dimer in a fashion such that it can interact with both monomers of the photosystem. PBSome rods (Figure 1.7B) employing the CpcG2 linker can also interact directly with PSI by a different mechanism, which allows preferential energy transfer to PSI rather than PSII. Other methods by which PBSomes can interact with PSI is directly via the APC core (Figure 1.7D) or by energy spillover to PSI while the PBSome is attached to PSII (Figure 1.7C). The last two mechanisms seem to be species specific (Mullineaux and Holzwarth 1993; Mullineaux 1994).

The most common mechanism by which PBSomes interact with photosystems in cyanobacteria is via direct energy transfer to PSII (Figure 1.7A). Previous research has shown that deletion of L_{CM} protein linking the APC to the

thylakoid membrane (i.e. CpcG2) prevents efficient energy transfer to PSI, effectively preventing state II transitions (Ashby and Mullineaux 1999). Also, deletion of ApcF (the β^{18} subunit interacting with the L_{CM} α-resembling subunit) and ApcD (an alternative α subunit) prevents energy transfer with both PSII and PSI (Ashby and Mullineaux 1999). In all cases, the PBSome interacts with both PSI and PSII on the stromal side of the thylakoid (Gantt and Conti 1965; Edwards and Gantt 1971).

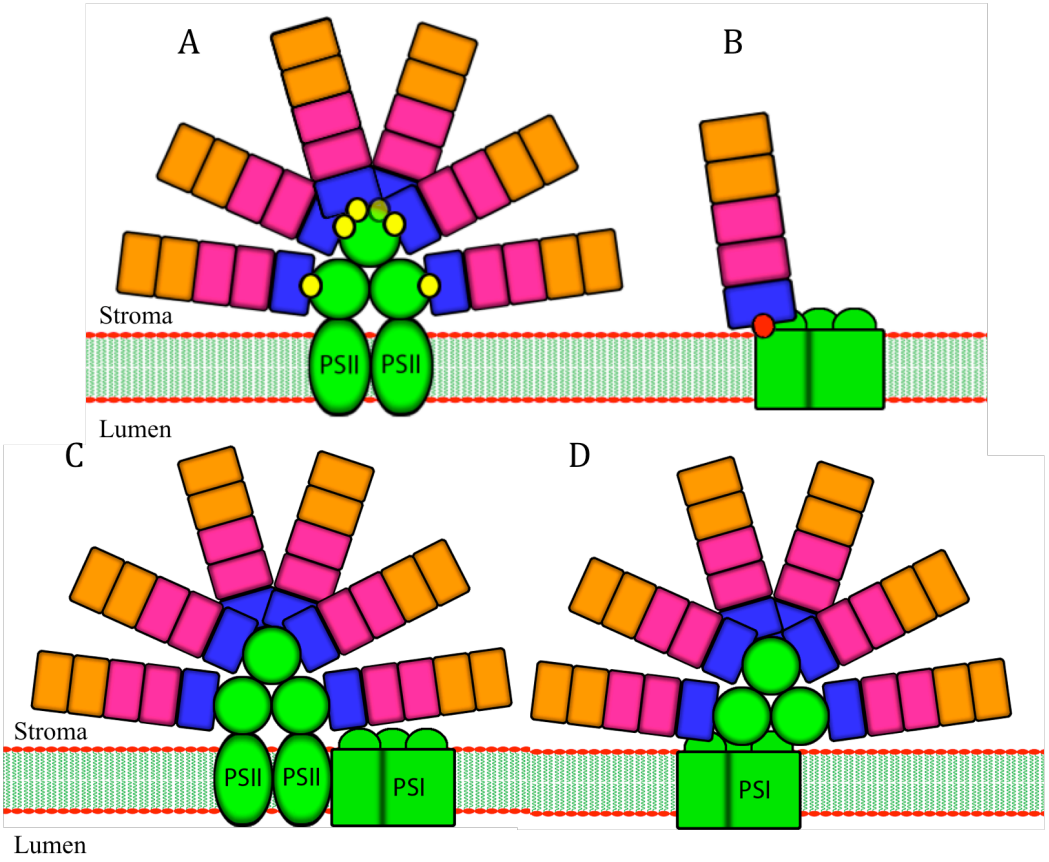


Figure 1.7: Methods for Phycobilisome Interaction with PSI and PSII in the Membrane. (A) The most common form of energy transfer involving PBSomes is between the APC core and PSII. Yellow circles represent CpcG1 L_{RC} linkers, and the PBSome color scheme is the same as in Figure 1.4. In (B), the rod structure is directly associated with PSI. Red circles represent CpcG2 L_{RC} linkers. (C) Energy "spillover" is reported as a method for PSI to receive energy from PBSomes. (D) In some instances, the APC of PBSomes may interact directly with PSI for successful energy transfer. Both C and D methods utilize the CpcG1 linker protein at the rod-APC interface.

Chapter 2: Design of a PSI-CpcG2 Fusion

1. Introduction

The inclusion of PBSomes to the Pt-PSI-utilizing hydrogen evolution system (cf. Chapter 1) requires both the isolation of PBSome rods separated from the APC and a subunit on PSI with which to associate. Naturally, sites on PSI for this type of association do not exist. *In vivo,* PBSomes interact optimally with PSI via the CpcG2 linker. However, the CpcG2 linker only associates with PSI under state-transition II light conditions. In order to replicate this interaction with efficiency, a PSI-CpcG2 fusion is the best option for success (Figure 2.1). Therefore, the desired system will combine PSI from *T. elongatus* to *Synechococcus* WH 8102 PBSome rods via a CpcG2 linker (also from the latter species) for improved hydrogen evolution. The rationale for the design of this PSI-CpcG2 fusion is discussed in the following sections.

2. Photosystem I Subunits

PSI is primarily responsible for the transfer of electrons from plastocyanin, a mobile electron carrier in the photosynthetic pathway, to FNR in the production of NADPH for reductive biosynthesis. The electron is first obtained by PSI from plastocyanin at the P700 reaction center, which contain a special pair of chlorophylls that absorb light maximally at 700 nm. The electron is subsequently excited to a higher energy state using captured light energy before continuing down the electron transport pathway to FNR. PSI can exist in monomeric or trimeric forms in cyanobacteria, though the trimer is more abundant (Rogner, Miihlenhoff et al. 1990). Each monomer of PSI contains twelve subunits,

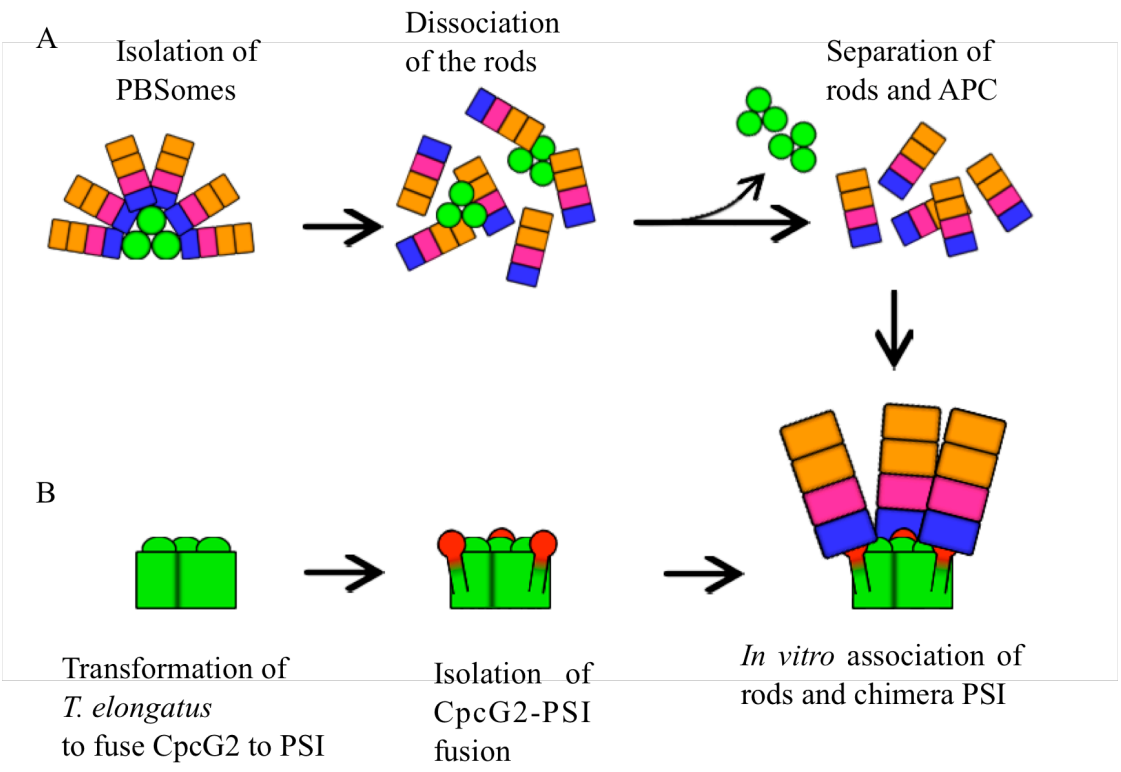


Figure 2.1: Design Scheme for the *In-Vitro* Association of Phycobilisomes to PSI. (A) Separation and isolation of the PBSome rods is a three step process starting with purification of the larger CpcG1 complex containing the APC core, dissociation of the rods, and separation of the rods from the APC. Combining the PBSome rod with PSI requires (B) transformation of the PSI through homologous recombination in *Thermosoynechococcus elongatus* to include a CpcG2 PBSome linker, isolation of this mutagenized PSI and *in vitro* assiciation of the PBSome rods to the chimera PSI.

coordinating 96 chlorophyll and 22 carotenoids accessory pigments. As previously discussed, PBSomes can interact directly with PSI for energy transfer. While CpcG1-bound PBSomes can successfully transfer energy to PSI, the CpcG2-bound alternative PBSome is capable of delivering energy to PSI at three times the efficiency (Ochiai et al. 2007). The interaction between PBSome rods and PSI has two characteristics to be addressed. First, the interaction between the two protein systems is transient (Busch, Nield et al. 2010), which is an undesirable quality for *in vitro* hydrogen production. Second, the production of CpcG2-bound PBSome rods and its interaction with PSI is dependent on growth conditions (Singh, Bhattacharyya-Pakrasi et al. 2009). The dependence on light quality can lead to low yields in protein isolation attempts unless an intentional effort is made to encourage CpcG2-bound PBSome formation.

Analysis of the structure and functionality of PSI leads to the identification of two potential sites where a fusion to CpcG2 can be made: PsaK and PsaX (Figure 2.2). Both subunits are found to be unnecessary for PSI trimer stability, and are neither required for activity of the P700 reaction center nor interactions with other proteins necessary for PSI activity (Grotjohann and Fromme 2005). Additionally, if the fusion with CpcG2 is successful, the subunits are spaced apart along the periphery of the PSI trimer allowing for enough room to potentially accommodate three PBSome rods (Figure 2.3).

2.a. PsaK

Crystallography at 2.5Å shows that PsaK is composed of a helix-loop-helix structure, with the loop located on the stromal side of PSI, and both N- and C-

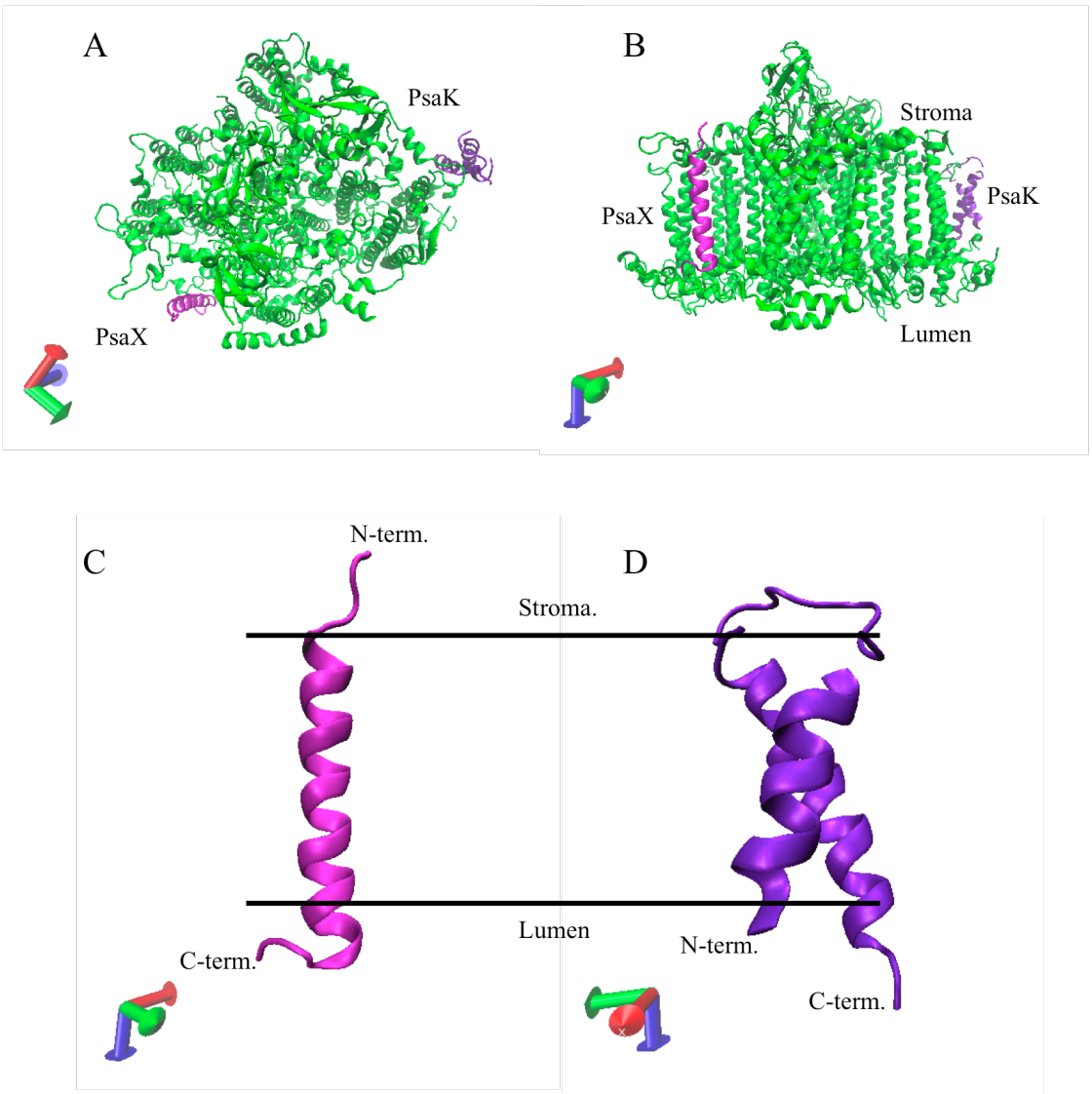


Figure 2.2: PsaX and PsaK in Photosystem I. (A) Top down view of the stromal side of a PSI monomer. (B) Side view of the outer surface of the PSI monomer. (C) PsaX (megenta) consists of a single transmembrane helix. (D) PsaK (purple) is shown as a helix-loop-helix with both N- and C- termini on the lumenal side of the thylakoid. [PSI PDB ID:1JB0, Jordan P. *et al.* (2001), *Nature,* 411: 909-917]

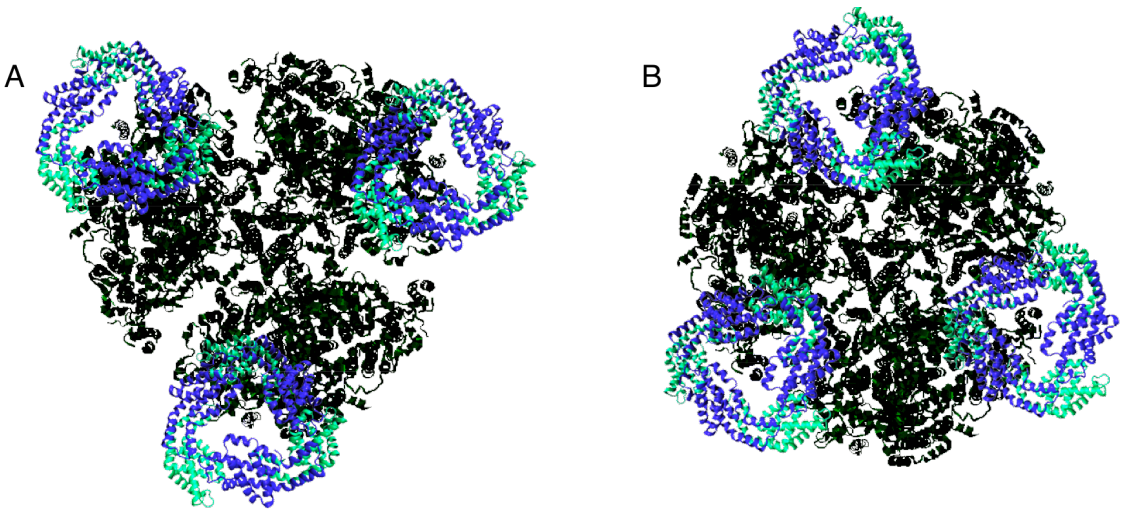


Figure 2.3: Projected Spacial Distribution of Phycobilisomes Attached to CpcG2-PSI Fusions. With either PsaX (A) or PsaK (B) fusions, the PBSome constructs are predicted to lack steric or other size-dependent restrictions with PSI (black) as shown. The distance between chosen PSI subunits and the addition of a flexible chain between the linker and PSI subunit should allow for PBSome binding at all three sites. PSI is shown in trimer form and oriented with the stromal side facing out. PBSomes are represented by a single PC trimer in blue and cyan. [PSI PDB ID:1JB0, Jordan P. *et al.* (2001), *Nature*, 411:909-917; PBSome PDB ID: 1B33, Reuter W. *et al.* (1999), *Proc. Natl. Acad. Sci.USA,* 96: 1363-1368]

termini on the lumenal side (Figure 2.2). PsaK only associates with PsaA, one of the primary components of the PSI reaction center (Fromme 2001). The PsaK subunit binds two chlorophyll molecules and connects to a carotenoid cluster. Genome-wide sequencing has revealed the presence of two forms of PsaK in certain organisms, named PsaK1 and PsaK2. Disruption of one or both PsaK-encoding genes shows no apparent change in PSI structure or activity, or on the organism's growth rates (Naithani, Hou et al. 2000). However, PsaK2 is required for effective state transitions in *Synechocystis* PCC 6803 (Fujimori, Hihara et al. 2005). Due to these characteristics, PsaK serves as a possible connection point to link PBSomes to the PSI apparatus *in vivo*, which could possibly translate to *in vitro* functionality if utilized in a PSI-CpcG fusion.

2.b. PsaX

PsaX is the last subunit of the cyanobacterial PSI to be identified and consists of a single transmembrane helix that lies along the periphery of the reaction center (Figure 2.2). This subunit is situated along the outer edge of the PsaB subunit and next to PsaF subunit of PSI. PsaX coordinates one chlorophyll molecule and two carotenoids. Currently, PsaX has only been found in thermophilic cyanobacteria, where it may be involved in stabilization of the PSI complex and interaction with accessory antennae systems (Grotjohann and Fromme 2005).

2.c. PSI subunit analysis

A PSI subunit with a stromal N-terminus is desired for the fusion since the CpcG2 will be fused at the C-terminus, as will be discussed in the proceeding

section. The crystal structure of PSI reveals that PsaX has a stromal N-terminus (Figure 2.2), and the amino acid sequence supports the latter by following the "positive inside rule," which predicts that the surface with a greater net positive charge will face the inside of the cell. Since the exact role of PsaX is still unknown, and it has no obvious function in PSI trimer stability, this subunit is assumed to be a safe location for fusion work. PsaK is also found to be a potential site for fusion work despite its lumenal side N-terminus. Mutations to PsaK showed that an independent C-terminal transmembrane helix is capable of insertion into the membrane, indicating that PsaK insertion is spontaneous and without the aid of chaperones or a translocation apparatus (Mant 2001). With the deletion of the N-terminal transmembrane helix, a fusion can also potentially be made at the PsaK subunit.

3. CpcG2: Additional Background and Analysis

As discussed earlier, CpcG2 is the alternative form of CpcG1, which is the rod-core linker responsible for the coupling of PC rods to the APC core. However, rather than connecting the rod to the core, the CpcG2 linker anchors the PBSome rod to the thylakoid membrane and facilitates the transfer of energy from the PBSome rod to PSI. Since the target PBSome for use in the proposed hydrogen evolution system will be from *Synechococcus* WH 8102, the CpcG2 variant from this organism will be used for fusion to PSI. In all organisms that possess a copy, the CpcG2 linker contains roughly 250 amino acids. Protein sequence alignments of CpcG1 (Figure 2.4) and CpcG2 (Figure 2.5) from the studied species reveal considerable conservation of the first 18 residues,

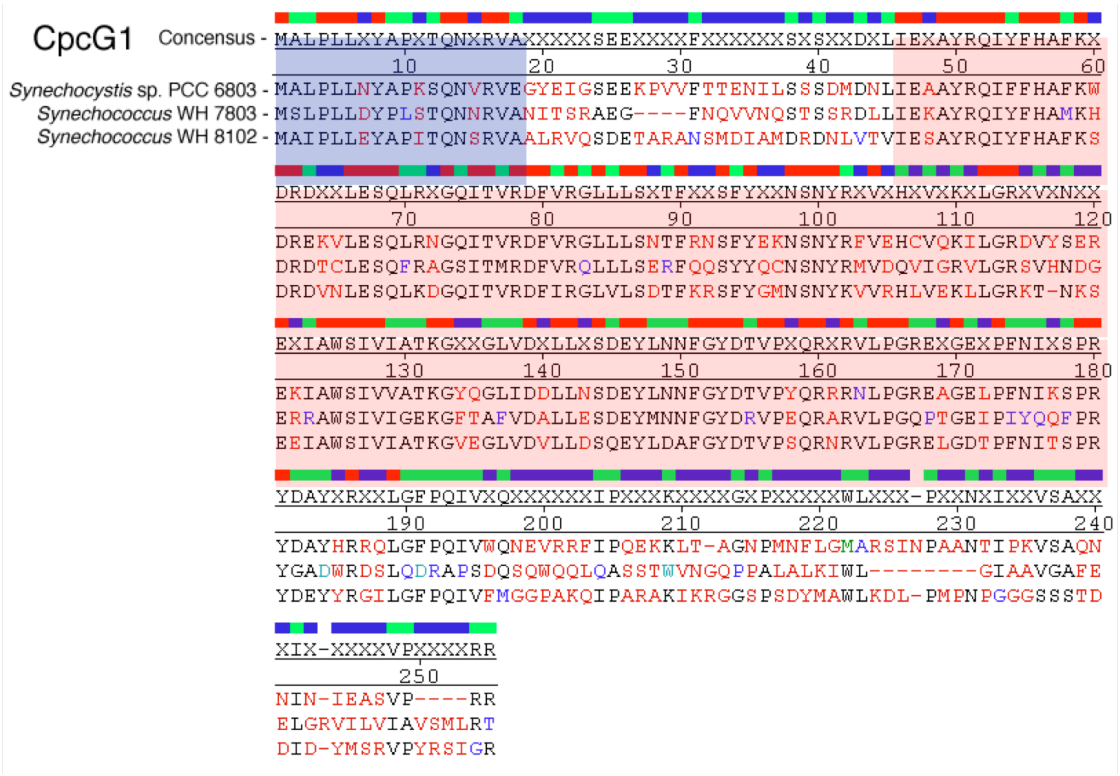


Figure 2.4: CpcG1 Protein Sequence Alignment. Two segments of the CpcG1 protein is highly conserved across tested species (and others not shown). Highlighted in blue is the N-terminus, and in red is the 'body' of the protein, which forms β sheets and interacts with the inside surface of a PC hexamer. The N-terminal region is hypothesized to interact with the C-terminus of the linker, which associates with the next distal PBSome subunit. The C-terminus is slightly hydrophilic in nature, but unconserved. The nature of interaction between the CpcG2 linker and the APC core of the PBSome complex is unclear.

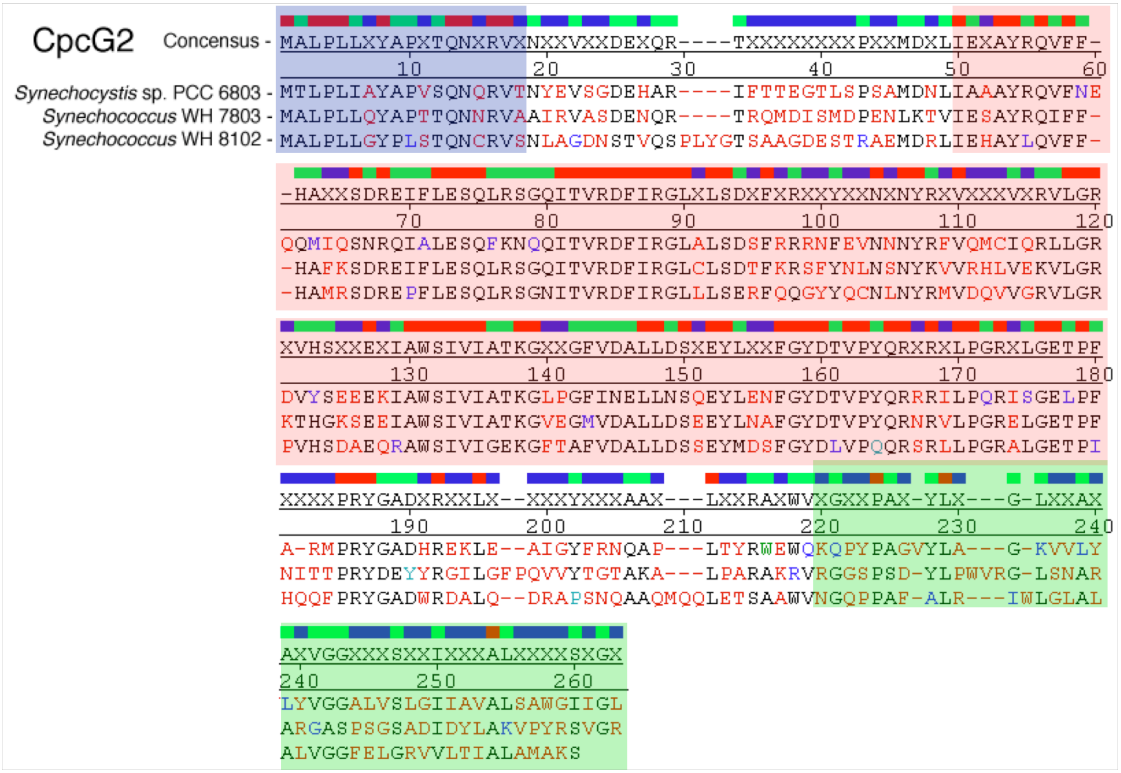


Figure 2.5: CpcG2 Protein Sequence Alignment. Similar to CpcG1, two segments of the CpcG2 linker are highly conserved across tested species (and others species not shown). The N-terminal region (highlighted in blue) is again hypothesized to interact with the C-terminus of the linker, which associates with the next distal PBSome subunit. Highlighted in red is the conserved β-sheet 'body' that interacts with the PC hexamer inside surface, and in green is the hydrophobic tail of CpcG2 that associates tightly with the thylakoid membrane. Aside from the hydrophobic nature of this region, the actual amino acid composition is not conserved.

followed by a variable region that continues to about residue 50. From residue 50-190 is another conserved region, beyond which is a hydrophilic or hydrophobic C-terminal region for CpcG1 or CpcG2, respectively (Figure 2.6). In total, these PBSome L_{RC} linkers can participate in three distinct interactions: the N-terminus and the variable region up to 50 amino acids is used for recognition by and interaction with the distal L_R linker; the conserved 'body' from residue 50-190 binds within the inner surface of the PBSome hexamer (or subunit) to which it coordinates; and the C-terminus is responsible for securing the hexamer to either the proximal core subunit or the thylakoid membrane in the energy transfer path. For CpcG1, the N-terminus of the linker can interact with the L_R linker from a distal PE subunit, while the conserved 'body' of the linker interacts with the PC subunit and its C-terminus connects the PC to the APC. In contrast, the C-terminus of the CpcG2 anchors the PC hexamer, and subsequent hexamers of the rod, to the thylakoid membrane.

Central to the design of the PSI-linker fusion is the desire to mimic *in vivo* energy transfer. The N-terminus of the CpcG2 linker, which helps coordinate the subunit composition of the PBSome rod, is important for binding of the distal rod subunit, so manipulation of this end is avoided. The C-terminus of this linker, while integral to thylakoid anchoring and PSI association, is of less importance to an *in vitro* hydrogen evolution system where the thylakoid membrane is absent. Therefore, the fusion of CpcG2 to PSI will be made at the C-terminus of the linker.

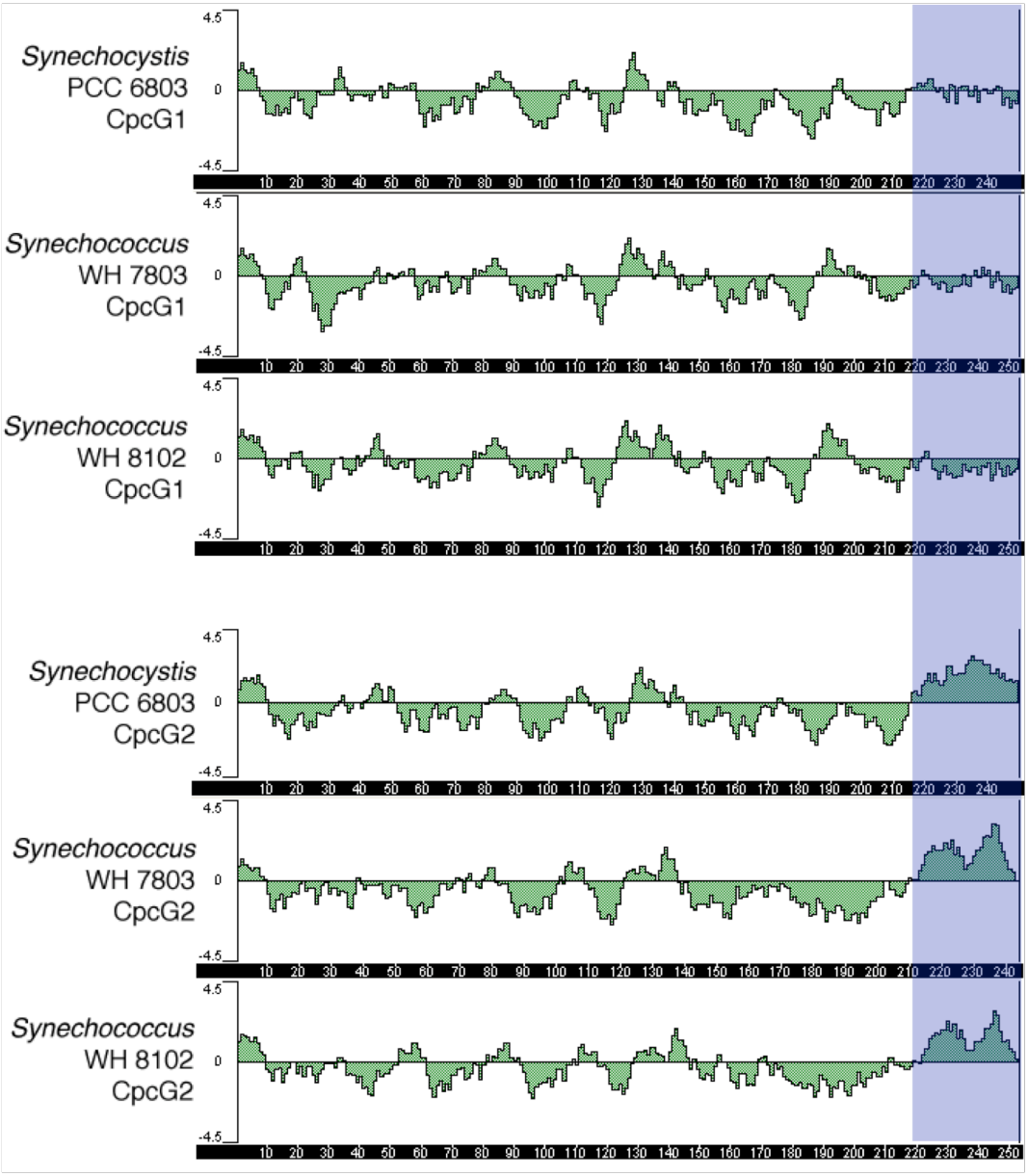


Figure 2.6: Hydropathy Plots for CpcG1 and CpcG2. The primary difference between CpcG1 and CpcG2 linkers is in the last 30-40 amino acids (highlighted in blue) of the C-terminus, which are hydrophobic in CpcG2, but slightly hydrophilic in CpcG1. Hydropathy plots are calculated using the Kyte-Doolittle calculation in Protean. The window size is 10 amino acids. Hydrophobic stretches of residues have a value above zero, while hydrophilic stretches are below zero.

4. Fusion Design

The desired system to increase the efficiency of hydrogen production is constructed upon the PSI isolated from *T. elongatus* to which the CpcG2 linker from *Synechococcus* WH 8102 is fused to promote PBSome rod association (Figure 2.7). To make successful mutations and incorporate the CpcG2 fusion in *T. elongatus*, homologous recombination is used, which requires the isolation of the PSI subunit genes plus flanking DNA and the appropriate restriction enzyme(s). The PsaK and PsaX encoding genes are isolated with 2 kbp of genomic DNA on either side. These genes, its flanking regions, and the gene for CpcG2 are searched for absent restriction sites. A number of blunt-cutting enzymes and a handful of staggered-cutting enzymes resulted from this search. Among the staggered-cutting enzymes are RsrII and its isoschizomers. [Originally, PsaJ was also considered for fusion and therefore included in this analysis, but later excluded due to concerns of its disrupting PsaF, and its subsequent interaction with PsaA and cytochrome (Grotjohann and Fromme 2005). Repeated analysis without PsaJ may yield additional enzyme options.] A HindIII site is also absent in the mentioned DNA sequences, but is reserved for the future addition of a kanamycin resistance gene to facilitate the selection of mutants. For this design, RsrII is chosen because of the 3-prime overhang it produces, which, if included in any of the target sequences, will not result in the introduction of undesirable residues at the site of fusion (cf. Appendix 6).

In the proposed design, the RsrII restriction site is inserted at the start of the PsaX gene in a way to ensure that the start methionine of the CpcG2 gene

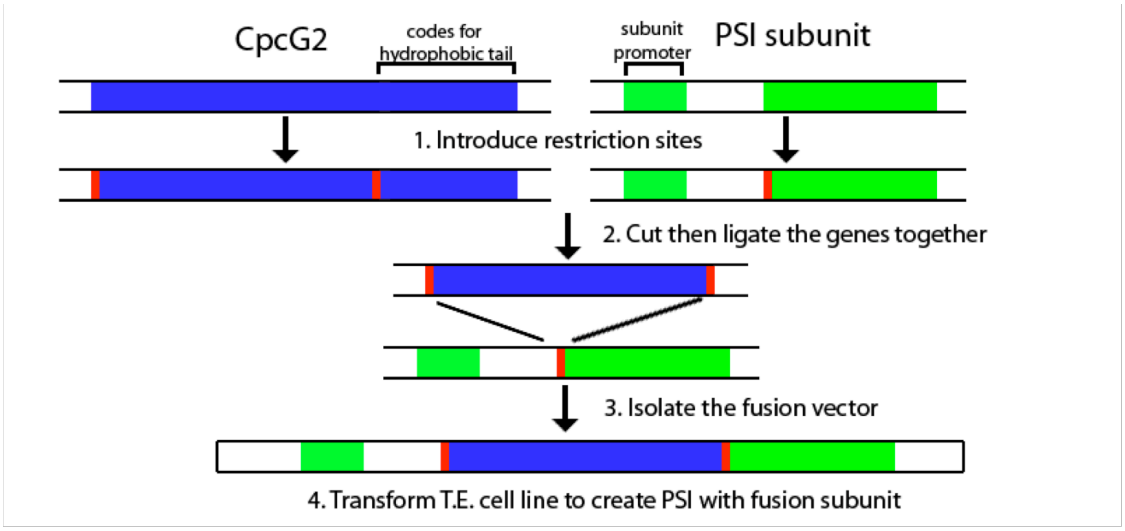


Figure 2.7: Molecular Biology Plan for Creating the CpcG2-PSI Fusion. The CpcG2 gene (blue) and PSI gene (green) are schematically represented above. Red bars represent restriction sites introduced via PCR. Restriction sites for RsrII are introduced via site directed mutagenesis. The portion encoding for the hydrophobic tail of CpcG2 is not necessary, and may even be detrimental to activity of the CpcG2-PSI fusion, and is thus excluded from the fusion design. The distance between the start methionine and the upstream promoter is preserved.

replaces that of PsaX and maintains its distance from the upstream promoter. In the PsaK construct, the N-terminal helix is omitted from the design to produce an N-terminal fusion site on the stromal side of PSI. This site for fusion is made by deleting the region in the PsaK gene encoding the first helix and inserting the RsrII site in a single step via PCR (c.f. Appendix 4 and 5 for all primers and PCR settings, respectively).

The CpcG2-encoding gene is extracted from *Synechococcus* WH 8102 with 2 kb flanking genomic DNA and inserted into a pGEM-T easy vector; subsequent sequencing results verified the success on this incorporation. The CpcG2 gene is then modified to insert a RsrII restriction site preceding the start methionine and at the end of the region encoding the conserved body of the linker. As an added feature to the fusion to facilitate movement of the CpcG2 linker and its eventual connection to the PBSome rod, a flexible spacer segment is created via four different reverse primers to incorporate a Ser-Ser-Thr repeat of various lengths (Table 2.1). The four truncated versions of the CpcG2 linker with flanking RsrII restriction sites plus a flexible space are created via PCR, and the products of the latter process are ligated into individual pGEM-T easy vectors.

Table 2.1: Construct Design for CpcG2 and a PSI Subunit. CpcG2 is designed to have a spacer between it and the PSI subunit after ligation. The spacer is a Serine-Serine-Threonine sequence and is repeated 0-3 times. The CpcG2 linker with various spacer lengths have all been created and are currently in a pGEM-T easy vector, ready for ligation with a PSI subunit.

	Desired Construct with Spacer
CpcG2-0spacer	CpcG2 - PSI subunit
CpcG2-1spacer	CpcG2 - SST - PSI subunit
CpcG2-2spacer	CpcG2 - SSTSST - PSI subunit
CpcG2-3spacer	CpcG2 - SSTSSTSST - PSI subunit

6. Location for HindIII Restriction Site and Kanamycin Resistance Drop-in

A thermostable form of the kanamycin resistance gene with flanking HindIII restriction sites can be inserted into the fusion construct vector to facilitate the selection of recombinant *T. elongatus*. The HindIII restriction site is absent in the PsaX and PsaK genes, as well as their flanking genomic regions. To find a location for the HindIII site insertion, a genome map (cf. Cyanobase: http://genome.kazusa.or.jp/cyanobase) is consulted to locate a site near the PSI subunit gene that will result in the least chance of having a negative effect on PSI. For PsaX, a site is found in a 55-base long region after its terminator sequence, which does not encode for any known or hypothetical protein, and does not appear to be a promoter sequence for any nearby genes. For these reasons, this region appears to be an acceptable location for the insertion of a kanamycin resistance gene.

Unlike PsaX, PsaK does not have a “safe” location for the kanamycin resistance gene insertion, as the end of the PsaK gene also encodes for another protein in the reverse direction. This encoding region (tll2274) codes for an unknown putative protein, which can potentially be modified with little or no negative effects due to the fact that the overlap of the two genes is minimal (i.e. 26 bases). If conservation of the putative domain is desired, the integrity of the gene can be preserved by repeating the overlap and creating a space between tll2274 and the PsaK gene where the kanamycin gene can be inserted. The latter is proposed for future work.

7. Statement of Research Goals

PSI, in conjunction with cytochrome and ascorbate, can be used to produce hydrogen in the presence of light. However, PSI is the only component in the system capable of capturing and using light in this process, primarily owing to the presence of chlorophyll pigments at the P700 reaction center where electrons are excited. Due to this pigmentation, PSI lacks the ability to absorb light across the visible spectrum, and thus is unable to utilize all incident white light. To improve the current hydrogen evolution design, PBSomes can be added to increase the light capturing efficiency of this system. However, only a specific part, the PBSome rod, is desired for this design, as it is capable of greater energy transfer efficiency to PSI than the whole complex. In addition to its isolation, a means to connect the PBSome rod to PSI is needed. In the proceeding work, the isolation of PBSomes is addressed, as is the dissociation of PBSome rods from the APC core, and progress on the PSI-CpcG2 fusion is presented. The ultimate goal is to investigate whole PBSome complexes, search for a method to decouple the interaction between the PC rods and APC core, and isolate individual PBSome rods for future attachment to PSI.

Chapter 3: Methods and Materials

1. PCR

For all fusion work, the pGEM-T easy vector (Promega, Fitchburg, WI) was used. All primers were purchased from Integrated DNA Technologies (Coralville, IA). Lyophilized primers were resuspended in autoclaved deionized water to 5*x* their working concentration and stored at -20ºC until further use. The DNA polymerase ExTaq (Takara Bio Inc., Shiga, Japan) was used in all PCR reactions. PCR reactions were performed in a Mastercycler Gradient Cycler, (Eppendorf, Hamburg, Germany) using the cycling conditions provided in appendix 5. Enzymes for restriction digestion (RsrII and HindIII) and ligation of PCR products (T4 ligase) were purchased from New England Biolabs (Ipswich, MA).

2. Transformation and Plasmid Isolation

The heat-shock transformation method was used to transform GC-5 competent cells (Genesee Scientific, San Diego, USA). Cells stored at -80ºC were thawed on ice. 100 ng of template DNA was added to the cells and the mixture was incubated on ice for 30 minutes. The cells were then heat-shocked at 45ºC for 45 seconds in a water bath and subsequently placed on ice for two minutes. 500 µl of room temperature SOC media was added to the cells, which were then incubated at 37ºC for one hour. Following incubation, 50-100µl of cells were inoculated on LB plates with the appropriate antibiotic for selection. X-gal and IPTG were also added to the plates for blue-white colony screening.

Colonies (white colonies, if blue-white screening was used) were picked, transferred to 5 ml of LB liquid medium, and incubated on a shaker for 10-14 hours at 37°C. Plasmids were subsequently purified from these cultures using a mini-prep kit (Wizard Plus, Promega, Fitchburg, WI).

3. Cell Culturing

Synechococcus WH 7803 and *Synechococcus* WH 8102 were grown in 2 L Nalgene bottles containing A+ and ASN media, respectively (see Appendix 3 for recipe). Growth took place at 25°C in an incubator with diffused continuous white light. Air was pumped in through a 0.2 µm diffuser at approximately 2 $L \cdot min^{-1}$. At low cell density, cultures were wrapped in a blue filter sheet.

Both *T. elongatus* BP-1 and *Synechocystis* PCC 6803 were growth in BG-11 media. *T. elongatus* BP-1 was cultured in a fermenter at 55°C with constant white light and air was bubbled through for both CO_2 diffusion and mixing. *Synechocystis* PCC 6803 was grown at room temperature with house air bubbling through a 0.2 µm diffuser.

All cells were harvested via centrifugation at 7,000g. The resulting pellet was resuspended with 750 mM Na/K-phosphate buffer (pH 7.8). If not used immediately for a PBSome purification prep, cells were centrifuged again and stored at -80°C.

4. Purification of Phycobilisomes

PBSome purification followed a previously published protocol (Gantt, Lipschultz et al. 1979) with some modifications. Purification was performed using

cell pellets previously rinsed with 750 mM Na/K-phosphate buffer (pH 7.8). Between 1 and 3 grams of cells were resuspended in 750 mM Na/K-phosphate buffer (pH 7.8; 10 ml buffer per gram pellet) and lysed via French pressure cell at 15,000 p.s.i. Triton X-100 was added at 3% and incubated on a rocker for 20 minutes at room temperature. To remove large cell debris, samples were centrifuged for 20 minutes at 20,000g, forming a pellet of cell debris at the bottom, followed by a supernatant and a detergent layer on top.

For *T. elongatus* BP-1, *Chroococcidiopsis* TS-821, and *Synechocystis* PCC 6803, the supernatant was removed and placed over a buffered sucrose step gradient with sucrose molarity at: 2.0 M (3 ml) 1.0 M (4 ml), 0.8 M (5 ml), 0.6 M (5 ml), and 0.4 M (5 ml). The gradients were centrifuged for 18 hours in a swinging bucket rotor (Beckman SW32-TI) at 18,000 rpm and 10°C. PBSomes were typically found at the interface between 1.0 M and 0.8 M sucrose, and were harvested using a syringe with a flat tipped needle.

In the case of *Synechococcus* WH 7803 and *Synechococcus* WH 8102, PBSomes were often retained in the detergent layer above the supernatant. In this case, the detergent was mixed with additional phosphate and layered over a buffered linear sucrose gradient. These gradients were spun under the same conditions as the step gradients mentioned previously. Gradients were fractionated and samples were tested with the Nanodrop ND-3300 for PBsomes integrity. Fractions with the most desirable fluorescence profile were kept for testing.

To concentrate samples, PBSomes isolated from *T. elongatus* BP-1 and

Synechocystis PCC 6803 were precipitated with 30% ammonium sulfate, resuspended in small volume of 750mM Na/K-phosphate buffer (pH 7.8), and dialyzed against the latter buffer. PBSomes isolated from *Synechococcus* WH 7803 and *Synechococcus* WH 8102 were mixed with 1.5 M phosphate to bring the buffered phosphate concentration to or above 1 M and force a salting out of the protein. Samples were then allowed to sediment for three days. The resulting phosphate supernatant was removed, and precipitated PBSomes were dialyzed against 750 mM Na/K-phosphate buffer (pH 7.8) and 1 M sucrose to achieve a homogenous resuspension.

5. Tricine-SDS-PAGE

The majority of PBSome components range between 14 and 100 kDa, with single peptides (e.g. L_{CM}) that can vary between 80 and 130 kDa in MW. Tris-tricine gels (Schagger, H. and G. von Jagow, 1987) were used to resolve the α and β subunits of the PBSome complex, as well as the linkers. These gels were made with the Protean-3 system (Bio-Rad) with a gel thickness of 0.75 mm. Electrophoresis of the gels was carried out at 100 V until the dye front either reached the bottom or ran off completely.

6. Absorbance Measurements

Purified samples were quantified by peak absorbance optical density with a Nanodrop ND-1000 spectrophotometer. The spectrophotometer was initially blanked with water. Absorbance spectra from 300-700 nm were subsequently collected. Absorbance peaks for blue PBSomes (from *T. elongatus* BP-1, and *Synechocystis* PCC 6803) are located at 624 nm. The peak for PBSomes

isolated from *Synechococcus* WH 7803 and *Synechococcus* WH 8102 are located at 545 nm and 495 nm, respectively.

7. Steady-State Fluorescence

For rapid preliminary inspection of complex integrity, samples were scanned with a Nanodrop ND-3300 to obtain an emission spectrum of the purified protein complex. Samples were excited using a blue LED to excite the most distal subunits of the PBSome rod structure. A dual-channel fluorometer from Photon Technologies Inc. was also used for fluorescence measurements. For analysis in the latter instrument, samples were diluted in 750 mM Na/K-phosphate buffer (pH7.8) to 0.1 OD_{peak} units and excited with light 10 nm blue-shifted from the sample's peak absorbance wavelength. Both excitation and emission slit-widths were set to 1 mm.

8. Stopped-Flow Fluorescence

Stopped-flow fluorescence was performed using an instrument provided by Bio-Logic, which is equipped with the MOS-450 monochrometer, a SFM-300 mixing unit, an 80 µl flow cuvette, and two photomultiplier tubes and bandpass filters. The mixing system and sample chamber were kept at 20°C using a water bath. The mixing system is equipped with four syringes capable of forced mechanical injection at desired ratios. A high-density-solution (HDS) mixing chamber was added to ensure homogeneity of the sample as it entered the flow cuvette. Samples at 5*x* the working concentration were added to the first syringe. Syringes two through four were filled with a phosphate buffer and/or water. Mixing ratios with a total of 20 units were used to achieve final phosphate

concentrations between 75 mM and 750 mM. Optical bandpass filters (Omega Optical, Brattleboro, VT) with peak transmittance at 680, 640 and 550 nm were used to monitor of APC, PC and PE fluorescence, respectively.

9. Chaotropic Dissociation Assay

The chaotropes used in this assay were either salt (NaCl) or urea. Equal volumes of solubilized PBSomes isolated from *Synechococcus* WH 7802 were aliquoted in a 96-well plate. These samples were diluted in a mixture of 750 mM Na/K-phosphate buffer (pH 7.8) and 3 M chaotrope (dissolved in latter buffer) to a desired concentration determined by a peak absorbance/OD_{545} of ~ 0.1 (see Appendix 2). Plates were shaken and allowed to incubate for one hour. Following incubation, the plates were spun at 5,000g for 30 minutes to pellet the insoluble protein. The samples were subsequently drawn from the supernatant for fluorescence analysis via the Nanodrop ND-3300 as previously described. All experiments were performed in triplicate.

10. pH Assay

Two separate pH studies were performed. The first studies were conducted on the blue PBSomes isolated from *Synechocystis* PCC 6803, *Chroococcidiopsis* TS-821, and *T. elongatus* BP-1. These samples were each aliquoted into five sample tubes and diluted with 750 mM Na/K-phosphate buffer that was titrated to a pH of 6, 6.5, 7, 7.5, and 8. (The buffer was prepared from and titrated in a 750 mM Na/K-phosphate monohydrate solution that had been filtered sterilized.) The samples were subsequently incubated in the dark for 30 minutes and then spun down at top speed. The resulting supernatant was removed and fluorescence

scans were collected on the Nanodrop ND-3300.

In a second test, 20 µl of the solubilized PBSomes (OD_{peak}= 4.0) purified from *Synechococcus* WH8102 were aliquoted into twelve tubes. 750mM Na/K-phosphate buffer at pH 7.8 and Na-K monobasic phosphate was added to create a pH gradient. The buffer pH was calculated using the Henderson-Hasselbalch equation:

$$pH = pK_a + log \frac{[base]}{[acid]}$$

Samples were incubated for 30 minutes with gentle agitation on an orbiter. Samples were then centrifuged at top speed for 1 minute. The supernatant was subsequently removed and its fluorescence measured in the Nanodrop ND-3300 fluorometer.

Chapter 4: Results

1. Progress in PSI-CpcG2 Fusion

The preliminary work completed towards the formation of the PSI-CpcG2 fusion involves modifying the CpcG2 gene isolated from *Synechococcus* WH8102 to have flanking RsrII restriction sites and a flexible spacer between its C-terminus and the chosen PSI subunit from *T. elongatus* BP-1. To accomplish the latter, a fragment containing the CpcG2 gene flanked by 2 kbp genomic DNA on both sides is amplified via PCR for ligation into the pGEM-T easy vector. Upon transformation, cells containing the ligated vector are inoculated onto LB plates for blue-white colony screening, and subsequently cultured in LB broth for amplification and isolation of the plasmid to verify the CpcG2 gene sequence. After verification of the integrity of the CpcG2 gene, PCR using four pairs of primers corresponding to the desired constructs (Table 2.1) is used to incorporate RsrII restriction sites and insert the Ser-Ser-Thr spacers. The four PCR products are then ligated into a pGEM-T easy vector and the desired constructs verified by restriction cutting and sequencing. As shown in Figure 4.1, successful modification of CpcG2 with the correct restriction sites and 0, 1, 2, or 3 sets of Ser-Ser-Thr spacers results in fragments that are 641, 650, 659, and 668 bases long, respectively, upon RsrII digestion. Thereby, the modification of CpcG2 for creation of a CpcG2-PSI fusion is completed.

For fusion to PSI, PsaX and PsaK are similarly isolated from *T. elongatus* BP-1 with 2 kbp genomic DNA on both sides and inserted into a pGEM-T easy vector (3 kbp). As seen in Figure 4.2, PsaX is successfully modified via-site

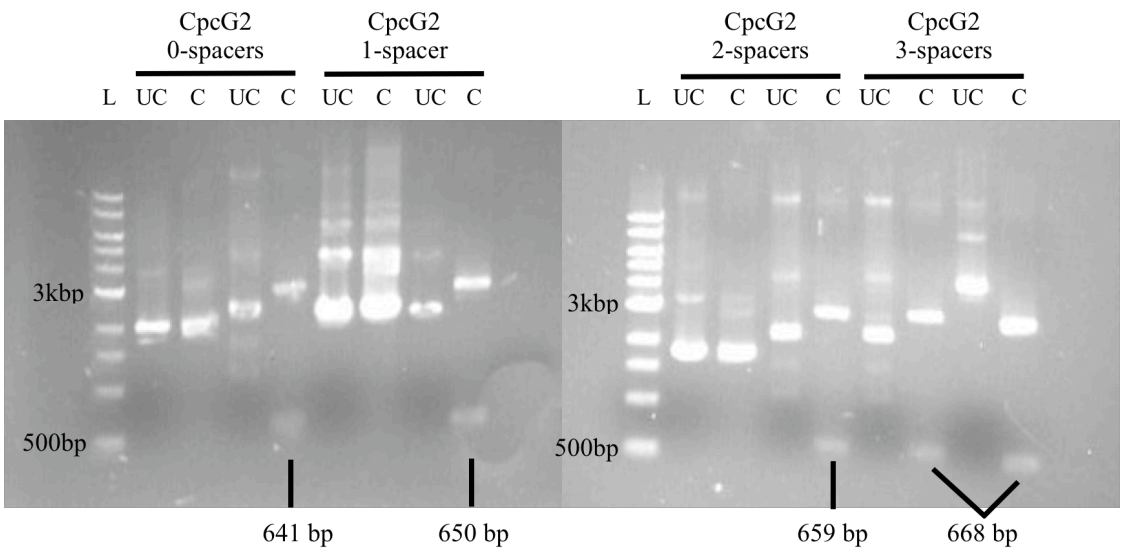


Figure 4.1: Agarose Gel of the CpcG2 Linker with Ser-Ser-Thr Spacer Sequences. Two colonies from each transformation are picked, cultured for plasmid purification., digested with RsrII, and analyzed by gel electrophoresis. Upon digestion, the CpcG2 gene with 0, 1, 2, and 3 spacer repeats are approximately 641, 650, 659, and 668 bp respectively. pGEM T-easy vector is 3,015 bp. Lanes marked 'L' are 1kb ladders, and UC and C represent 'uncut' and 'cut' samples, respectively.

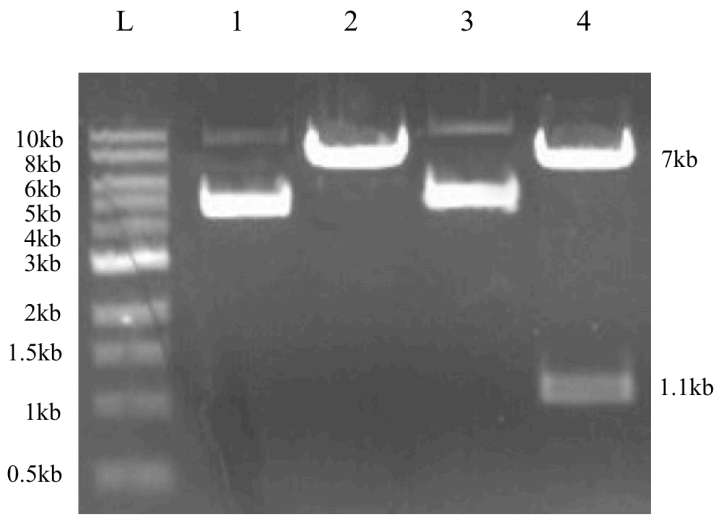


Figure 4.2: Modified PsaX Digested with RsrII and HindIII. Lane 1 shows uncut PsaX modified with an RsrII and HindIII with 2 kpb flanking genomic DNA in a pGEM-T easy vector (~3 kbp). In lane 2, the PsaX plasmid is cut with RsrII to produce a band at 7 kbp. Lane 3 contains uncut PsaX with the kanamycin resistance gene in the pGEM-T easy vector, while lane 4 contains the digestion products of the latter with HindIII to excise anamycin resistance gene (1.1kbp) from PsaX (7 kbp). Lane 'L' is a 1 kbp ladder.

directed mutagenesis to have both RsrII and HindIII restriction sites at the necessary locations. Insertion of a thermo-tolerant kanamycin resistance gene (1.1 kbp) at the HindIII site is also completed, and verified via cut-check. Ligation of the CpcG2 with various spacers to the modified PsaX and work on PsaK modification is pending.

2. Phycobilisome Isolation

The last step in purification of the PBSomes is ultracentrifugation of the cell lysate over a sucrose gradient. Upon centrifugation, the top of the gradient is occupied by a detergent layer formed by Triton X-100, which is dark green in color, indicating the presence of chlorophyll and chlorophyll-containing proteins (e.g. PSI & PSII) (Figure 4.3). Directly below the detergent layer, dissociated PBSome pieces, sometimes forming discrete bands, are found. Whole PBSome complexes, though different in color from organism to organism, are located in the lowest translucent band. Below this band is the cell lysate not solubilized by the detergent.

The lowest translucent band containing the PBSome complex is extracted from the sucrose gradient and analyzed by gel electrophoresis to check for purity (Figure 4.4 and Figure 4.5). To this respect, Tris-Tricine gels are advantageous to use to separate the small components of the PBSome structure. In these gels, the small rod-capping linker protein occasionally produces a weak band that is observed at ~ 9 kDa (not shown). Typically, the smallest bands seen on the gel are the α and β subunits at approximately 21 kDa. These subunits from different hexamers that comprise the PBSome are indistinguishable from each other in

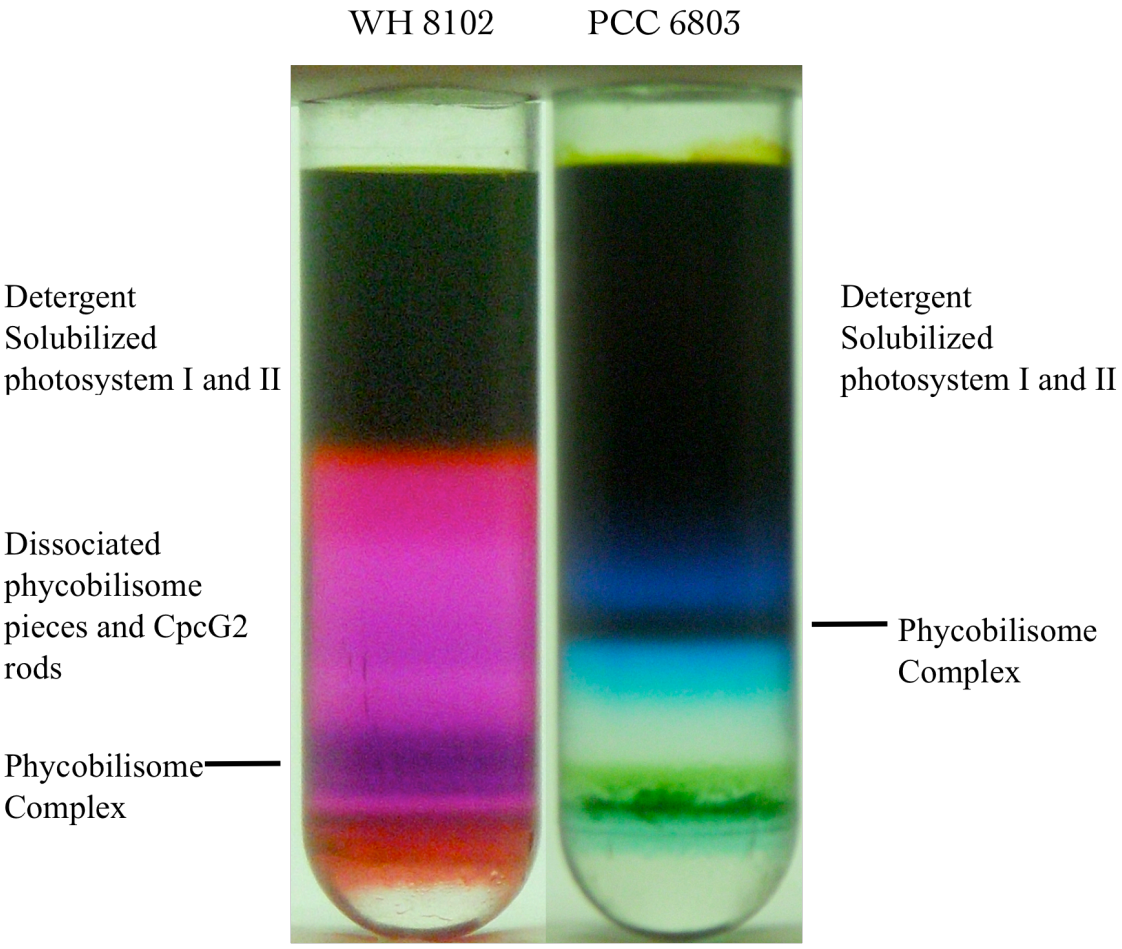


Figure 4.3: Purification of Phycobilisomes on a Sucrose Density Gradient. The lowest translucent colored band is the PBSome complex. Below that at the 2 molar sucrose interface is cell lysate no solubilized by the detergent/s. The difference in location of the two PBSomes shown is due to the difference in size of the complex. PBSomes isolated form WH 8102 and WH 7803 (not shown) will settle further down the gradient because the rods are comprised of an increased number of hexamers than the rods found in PCC 6803.

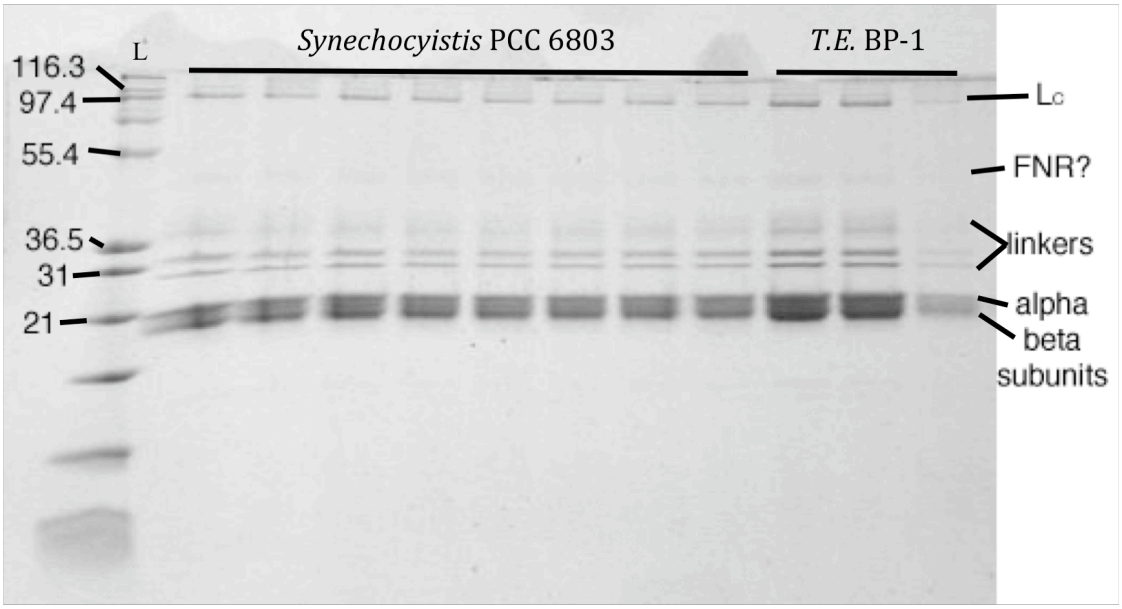


Figure 4.4: Tris-Tricine Gel Electrophoresis of Blue Phycobilisomes. Samples from various PBSome purifications are analyzed by SDS-PAGE. Band profiles for both organisms in the gel show little difference in protein composition or molecular weight of subunits. Lane 'L' is the Invitrogen Mark12 ladder.

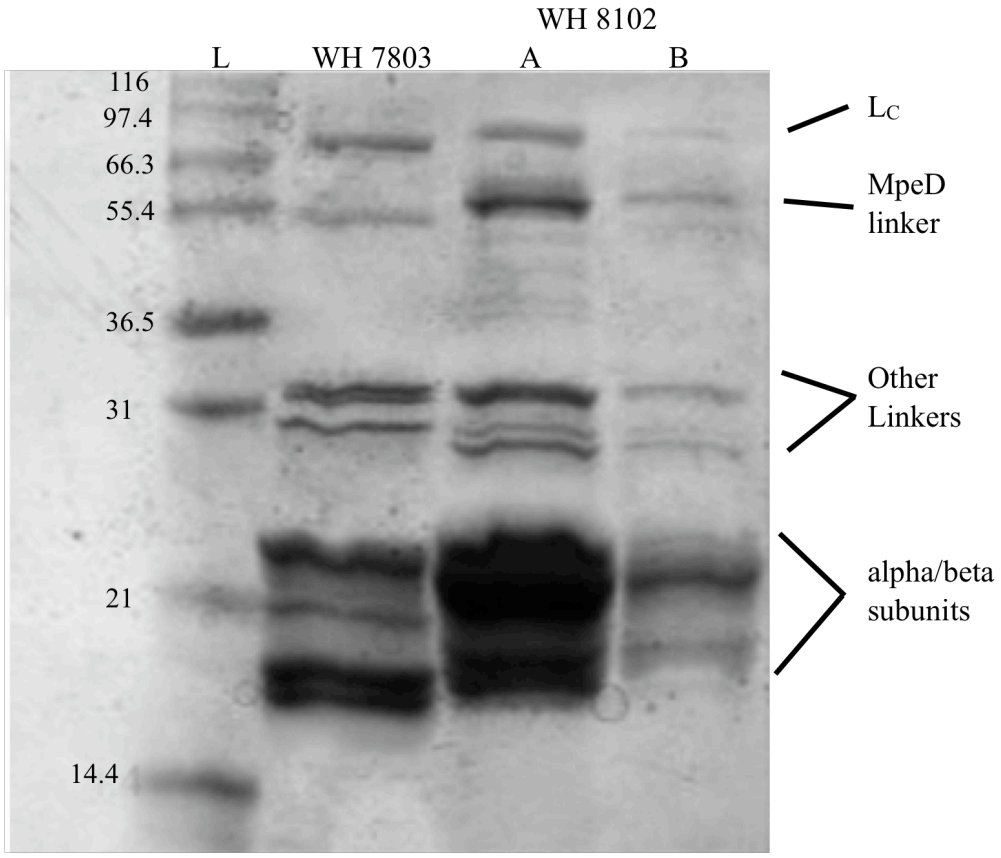


Figure 4.5: Tris-Tricine Gel Electrophoresis of Phycobilisomes Isolated from *Synechococcus* WH 7803 and *Synechococcus* WH 8102. The isolated PE-containing PBSomes used for the dissociation studies are shown here. The bands observed between 36.5 kDa and 55.4 kDa in the lane WH 8102A are thought to be FNR (Six, Thomas et al. 2007).

most gel systems. Directly above the α and β subunit are bands corresponding to the various linkers that are employed to maintain the structural stability of the PBSome rods and APC core. A band for FNR_L co-purified with the PBSomes may also be present over these linker bands. Since the FNR_L attaches itself to the PBSome in the latter case, separation of FNR_L is not achievable through the published purification method of PBSomes cited. Another method for its separation is needed, but does not currently exist. At roughly 59 kDa, the next large band for *Synechococcus* WH 7803 and *Synechococcus* WH 8102 is the MpeD linker (also called the Ƴ-linker). At the top of these gels, a band that contains the largest protein, the L_C linker, is present.

Recombinant PBSome rods can be isolated independently from the rest of the PBSome complex, but only at low yields. In order to obtain the rod structure in large quantities, purified whole PBSomes are investigated to search for a method by which rods can be separated from the APC core.

3. Dissociation of Phycobilisomes

3.a. Chaotropic Dissociation of Phycobilisomes

To identify dissociation pathways and search for conditions that allow for targeted dissociation of PBSome rods from APC cores, chaotropic dissociation of PBSomes (Figure 4.6 and Figure 4.7) is attempted and observed by fluorescence spectroscopy. Two chaotropes, sodium chloride (NaCl) and urea [$CO(NH_2)_2$], are chosen for this study based on their mechanism of protein destabilization and solubility in a 750 mM Na/K-phosphate buffer at pH 7.8. NaCl is selected for this study because of its previously established ability to remove PBSomes in the

purification of PSI. In PSI purification, after lysis of cyanobacterial cells, the thylakoid membrane must be washed with 3M NaCl to prevent PBSomes co-purification with PSI. The high salt acts by way of electrostatic shielding of charged particles, preventing ionic interactions, which are essential to non-covalent protein interactions (Tobias and Hemminger 2008). In addition, urea is similarly chosen for the dissociation studies because of its well-characterized ability to compete for hydrogen bonding and affect the solvent shell around protein structures (Timasheff and Xie 2003).

As mentioned previously, the APC core has an emission maximum at 680 nm, while the PC and PE have emission maxima at 655 nm and 560 nm, respectively. Under both chaotropic conditions shown in Figure 4.6A and Figure 4.7A, the results reveal a gradual shift away from APC fluorescence towards emission by PC, and ultimately by PE, as the concentration of the chaotrope increases. These changes are shown more clearly in normalization of the spectra in Figure 4.6B and Figure 4.7B.

The fluorescence of each PBSome functional subunit (PE, PC and APC) is plotted versus salt concentration (Figure 4.6C) to obtain the ratio of PC:APC and PE:PC. The former fluorescence intensities are taken at the shoulder of the maximum emission due to the overlap of the gaussian curves, while the PE fluorescence intensity is taken at the maximum emission. The ratio values as a function of salt concentration are shown in Figure 4.6D. Between 0.1 and 0.6 M NaCl, the PC signal increases with respect to APC, while the PE:PC signal

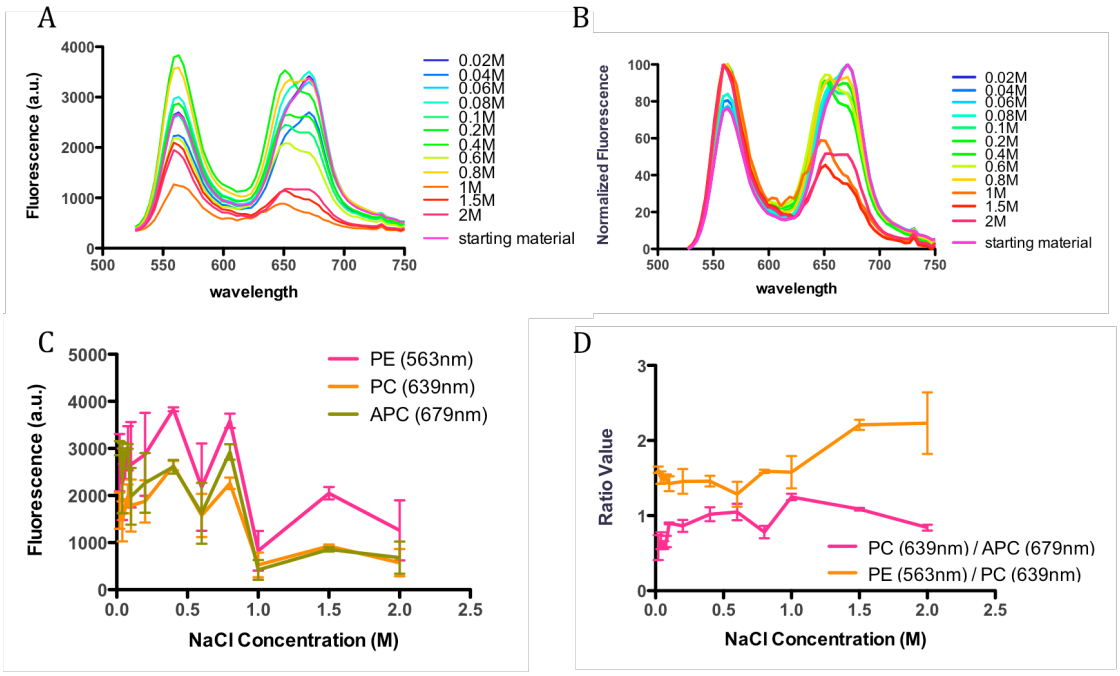


Figure 4.6: Chaotropic Dissociation of Phycobilisomes in the Presence of NaCl. Under increasing NaCl concentrations, PBSome dissociation is observed via fluorescence by excitation at 460 nm, and measuring the fluorescence emissions from 525 - 750 nm. (A) The emission spectra of PBSomes exhibit changes in intensity of the ACP, the PC, and the PE signals with respect to salt concentration, and are (B) normalized to elucidate the shift in signal from the APC to the PC and PE subunits. (C) Plotting independent values for functional the PE, PC, and APC versus salt concentration, along with (D) the ratios of its fluorescence, helps identify possible conditions for targeted dissociation.

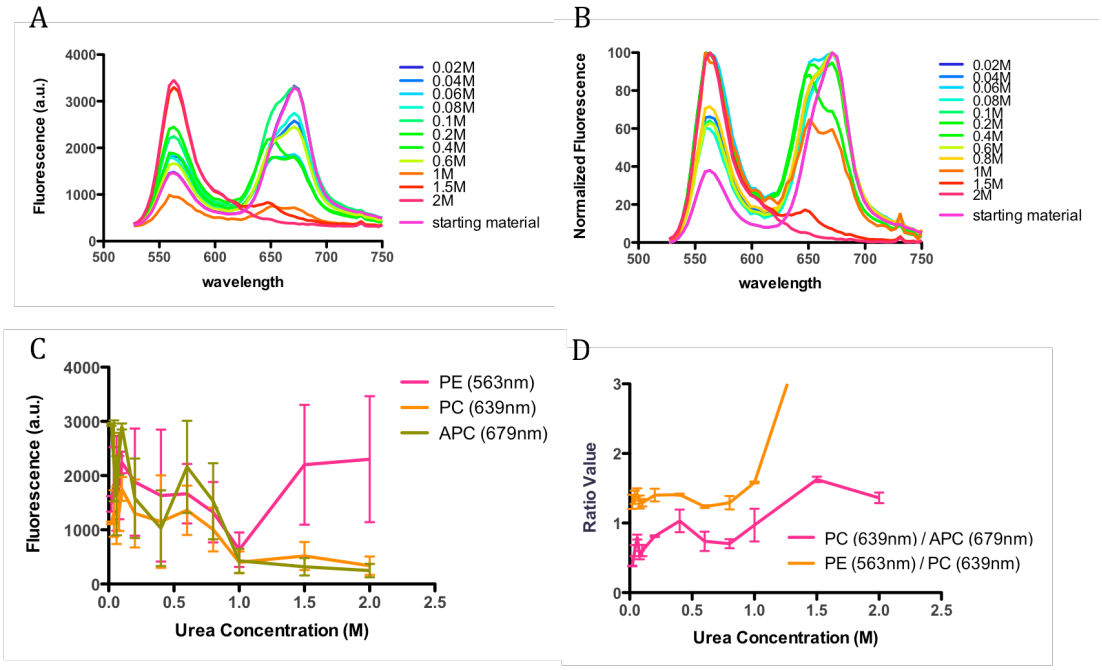


Figure 4.7: Chaotropic Dissociation of Phycobilisomes in the Presence of Urea. Under increasing urea concentrations, PBSome dissociation is observed via fluorescence by excitation at 460 nm, and measuring the fluorescence emissions from 525 - 750 nm. (A) The emission spectra of PBSomes exhibit changes in intensity of the ACP, PC, and PE signals with respect to urea concentration, and are (B) normalized to elucidate the shift in signal from the APC to the PC and PE subunits. (C) Plotting independent values for functional PE, PC, and APC versus salt concentration, along with (D) the ratios of its fluorescence, helps identify possible conditions for targeted dissociation.

remains constant. At 0.8 M NaCl, there is a depression in all PBSome signals, and above 0.8 M NaCl, an increase in the PE signal is observed, while the PC and APC fluorescence remains low.

Fluorescence data from PBSomes disassociated in urea yielded noisier data overall in comparison to the NaCl dissociation results. In the normalized spectra (Figure 4.7B), the fluorescence of the PBSomes in the presence of 0.02 M urea resembles the starting material. Above 0.02 M urea, the PE signal increases sharply with respect to the fluorescence emission from the PC and APC. From 0.04 M to 0.1 M urea, the PC signal gradually increases with respect to APC fluorescence, while the PE signal remains proportional to the peak value at PC and/or APC. Above 0.6 M urea, the largest change in fluorescence is from PE, while the PC and APC signals begin to decline. The latter trend continues until the urea concentration reaches 2 M. The ratio plot (Figure 4.7D, derived from Figure 4.7C) shows the relative fluorescence signals of PE in relation to PC, and the PC with respect to the APC signal. From 0.2 M to 0.4 M urea, the PC:APC ratio value increases, while the PE:PC ratio value remains constant. Above 0.8 M urea, both ratios begin to move upward together, but beyond 1M urea, the increase in PE:PC signal outpaces the change in the PC:APC signals.

3.b. Low Phosphate Dissociation of Phycobilisomes

Phosphate buffer at a concentration of 750 mM phosphate is typically used for the maintenance of PBSome structure due to its ionic strength, which encourages tighter hydrophobic interactions within the PBSome to keep the

complex together (Zilinskas and Glick 1981). By decreasing phosphate concentration, phycobilisome dissociation is promoted without the addition of chaotropes or other outside forces. Thereby, the disassociation of the *Synechocystis* PCC 6803 and *Synechococcus* WH 8102 PBSomes is observed, as shown in Figure 4.8 and Figure 4.9.

The results from the low phosphate dissociation tests on PBSomes isolated from *Synechocystis* PCC 6803 are shown in Figure 4.8. These PBSomes only contain the PCB chromophore, simplifying their excitation and emission spectra. With excitation at 550 nm, only PC chromophores are excited, guaranteeing that the APC will only fluoresce if the PC successfully transfers energy to it. Emissions from the PC at 640 nm and the APC at 690 nm are monitored by stopped-flow fluorescence to achieve low phosphate conditions by dilution of the 750 mM Na/K-phosphate with water and rapid mixing. As shown in Figure 4.8A and Figure 4.8B, the PC signal increases as the APC signal simultaneously decreases, which is expected when the PC dissociates from the APC. The inverse signal changes are interpreted as disruption of energy transfer between the PC and APC. This change, however, can not be used to identify the dissociation of the individual PC hexamers that comprise the rod, as each PC monomer is assumed to give off the same wavelength of emission, and therefore cannot be distinguished from one another. Despite the latter, we can successfully monitor the interruption of energy transfer to APC, and the apparent dissociation half-lives do, in fact, function on a predictable exponential basis with phosphate concentration (Figure 4.8C).

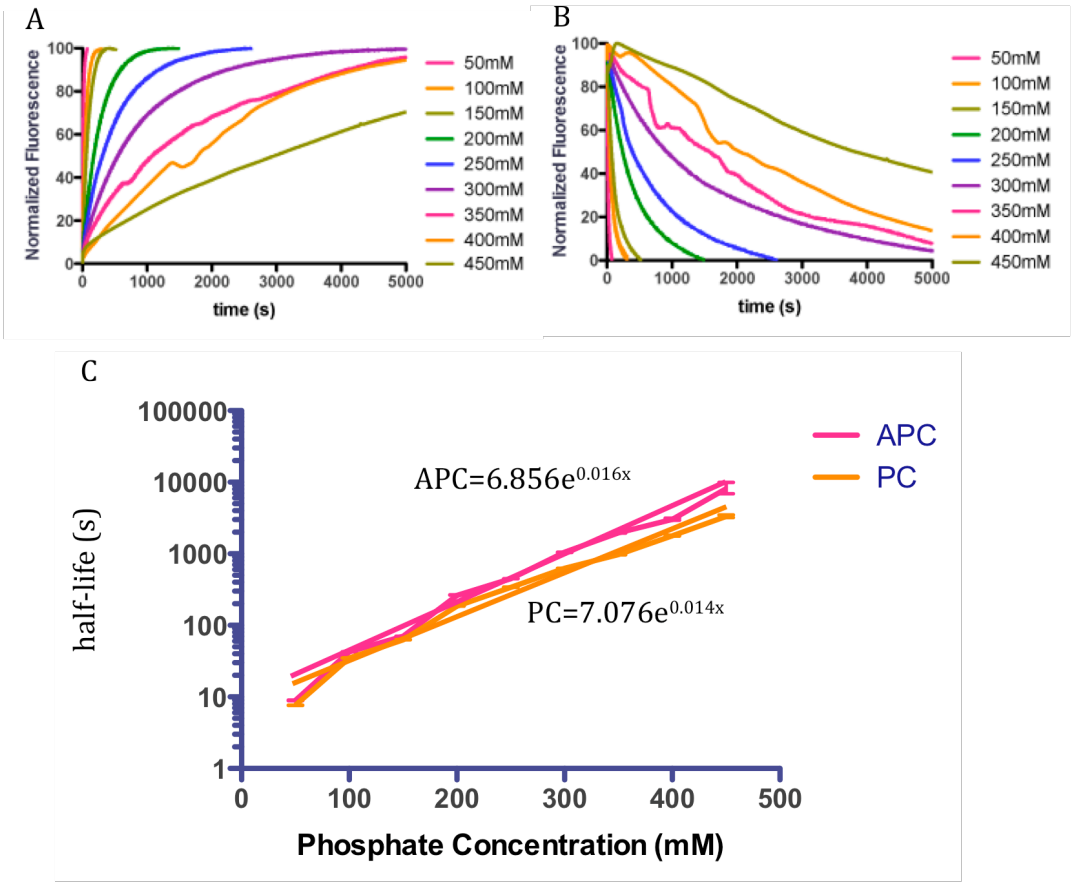


Figure 4.8: Low Phosphate Dissociation Kinetics of Phycobilisomes Isolated from *Synechocystis* PCC 6803. Stopped-flow fluorescence is used to measure (A) the PC and (B) APC subunits emissions at 640 nm and 690 nm, respectively. (C) Fitting of the curve to a first exponential decay yielded half-lives that are plotted on a logarithmic scale against phosphate concentration. The added trendlines show an exponential correlation between phosphate concentration and fluorescence half-lives. The experimental phosphate concentrations ranged from 50 mM to 450 mM with 50mM steps in between. (Samples in 750 mM phosphate are not shown, as a measurable change in fluorescence does not occur.)

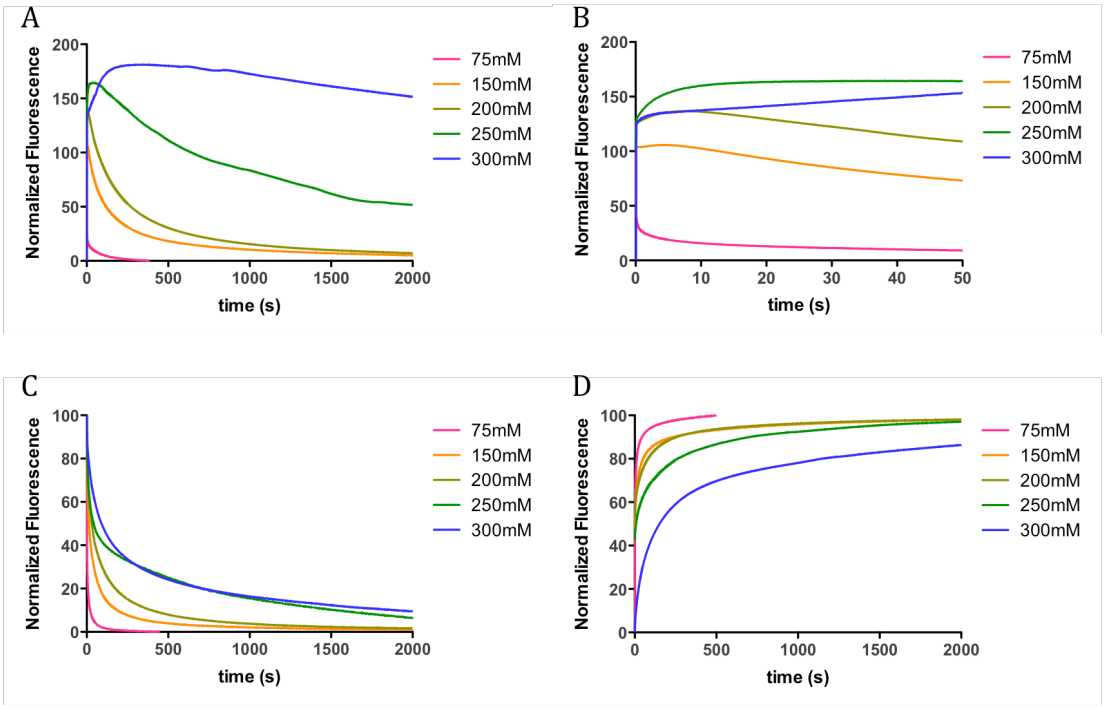


Figure 4.9: Low Phosphate Dissociation Kinetics of Phycobilisomes Isolated from *Synechococcus* WH 8102. (A,B) Via stopped flow fluorescence, the emission signals of the PC subunit measured at 640 nm and plotted as a function of time are shown in a set at two different time scales. (C) The APC and (D) PE subunit fluorescence emissions are measured at 690 nm and 550 nm, respectively, over time. Signals are normalized to the first and last data points in each series. The excitation wavelength is set to 480 nm to ensure that only PE subunits are excited.

The low-phosphate dissociation experiments with PBSomes isolated from *Synechococcus* WH 8102 are shown in Figure 4.9. Dissociation conditions for the latter are changed slightly to account for the characteristic differences between the PBSomes (to be discussed later). Bandpass filters are used to monitor light intensities at 550 nm, 640 nm, and 690 nm to capture emissions from the PE, PC, and APC, respectively. The APC signal at 690 nm changes similarly to the APC signal from *Synechocystis* PCC 6803 (Figure 4.9C). As time increases, this signal decreases, indicating a loss of energy flow toward the APC, which can be interpreted as PBSome dissociation. The PE signal at 550 nm increases with time similar to the PC signal of *Synechocystis* PCC 6803. (Figure 4.9D) Since this subunit is being excited by the light source, when fully dissociated, the PE will be the only component to fluoresce. The PC signal at 640 nm is the most interesting to this study because, as dissociation begins, this signal first exhibits an increase in intensity followed by a slow decrease (Figure 4.9A and Figure 4.9B). The latter behavior can be described by an initial dissociation at the PC-APC interface to form independent rods, followed by the dissociation of the rods into its individual structural components.

3.c. pH Dissociation of Phycobilisomes

PBSomes from *Synechocystis* PCC 6803, *Chroococcidiopsis* TS-821, *T. elongatus* BP-1 are incubated under different pH conditions to determine if dissociation of the complex occurs in a pH dependent fashion. Other studies of PBSomes from *Porphyridium* and *Nostoc* showed some degree of dissociation with a change in pH (Zilinskas and Glick 1981; Anderson, Rayner et al. 1983).

The pH dissociation of the PBSomes is tested by fluorescence, with excitation at 540 nm to excite the PC rods and monitor its energy transfer to the APC. As shown in Figure 4.10, a steady blue-shift in the fluorescence signal is observed for all PBSomes tested as the pH is decreased from 8 to 6, indicating a loss of energy transfer from the PC to the APC. For *Synechocystis* PCC 6803 (Figure 4.10A and Figure 4.10D), the change in signal does not start until the pH is dropped to 6.5, while the *Chroococcidiopsis* TS-821 (Figure 4.10B and Figure 4.10E) and *T. elongatus* BP-1 (Figure 4.10C and Figure 4.10F) show a slight blue-shift beginning at pH 7. Normalization of the emission scans (Figure 4.10D, Figure 4.10E, and Figure 4.10F) removes changes in intensity, making it easier to see the blue-shift with respect to pH. A slight increase in the fluorescence signal is also observed in each case, and may be either [1] an indicator for dissociation of the rod structure into independent PC hexamers, each capable of fluorescing independently, or [2] caused simply by the dissociation of the rods from the APC. Assuming near 100% efficiency in energy transfer in PBSomes and conservation of energy within the PBSome, the former explanation seems more likely to cause the increase in signal observed than the latter.

Similar to the blue PBSomes, the pH dependent dissociation is tested on PBSomes isolated from *Synechococcus* WH 8102 (Figure 4.11). In this experiment, sucrose is intentionally left out from the buffers to encourage the PBSomes to precipitate when in the full complex. The latter is not possible in the previous tests, as the blue PBSomes exhibit a greater solubility in 750 mM phosphate than the *Synechococcus* WH 8102 PBSome, and do not have

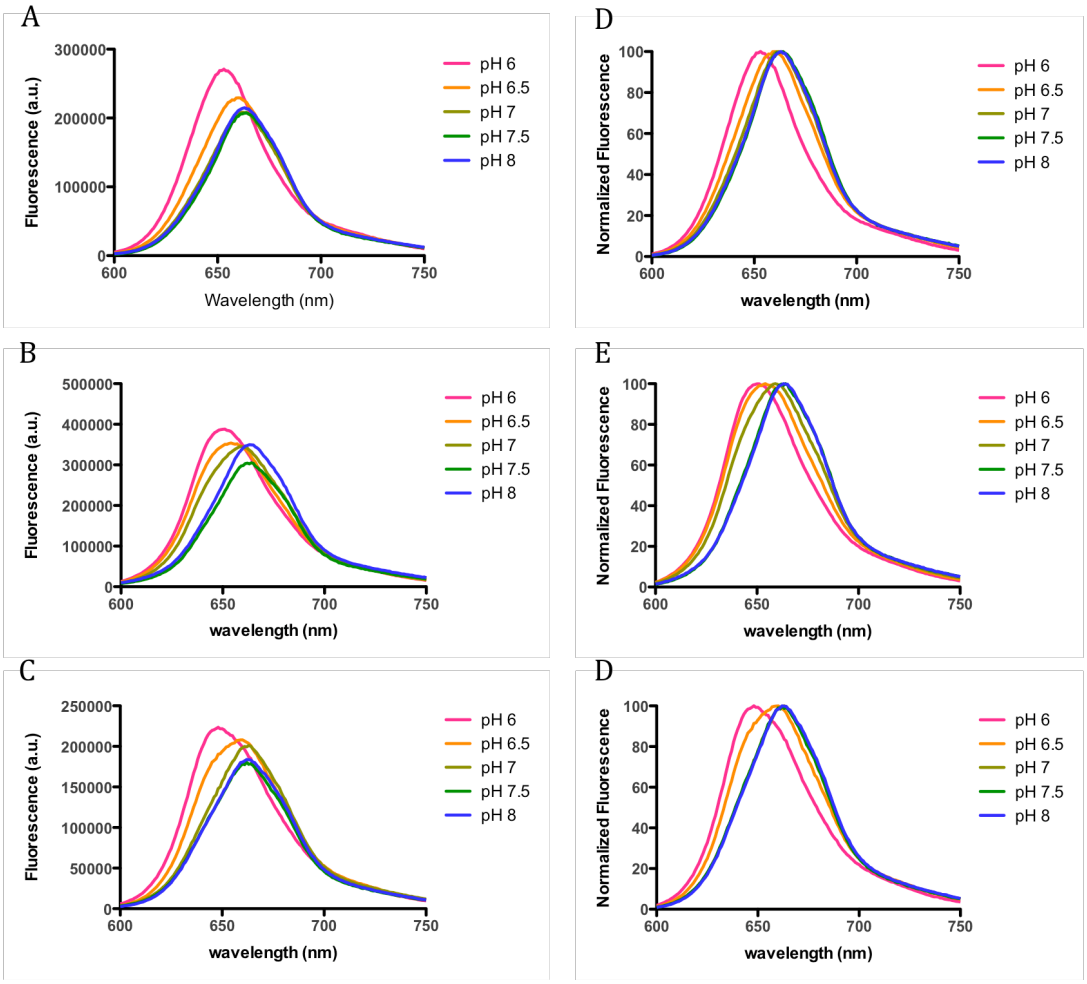


Figure 4.10: pH-Dependent Dissociation of Blue Phycobilisomes. Fluorescence spectra of PBSomes isolated from *Synechocystis* PCC 6803 (A, D), *Chroococcidiopsis* TS-821 (B, E), and *T. elongatus* BP-1 (C, F) after incubation in a 750 mM phosphate buffer under different pH conditions. Emission scans are shown in the left panels and normalized values in the right panels.

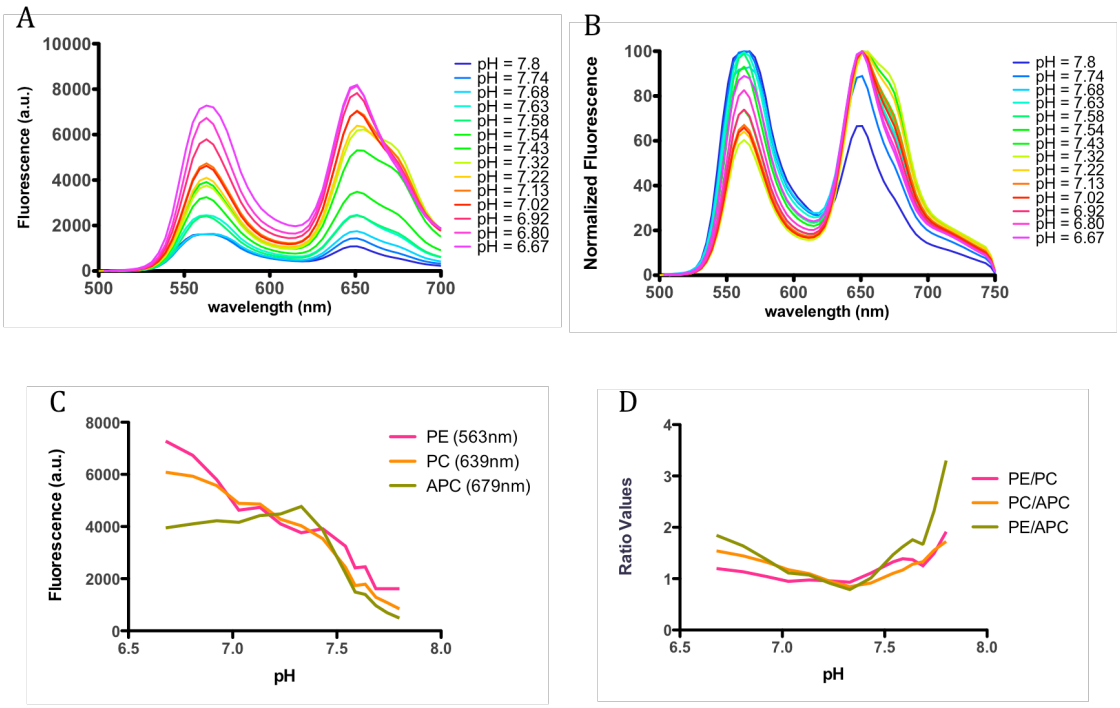


Figure 4.11: pH-Dependent Dissociation of Phycobilisomes Isolated from *Synechococcus* WH 8102. In this experiment, PBSomes from *Synechococcus* WH 8102 are incubated under different pH conditions, excited at 480 nm, and the emission spectra (A) from 500-700 nm is collected and (B) normalized to their peaks. (C) The fluorescent signals from the PE, PC, and APC subunits at 563 nm, 639 nm, and 679 nm, respectively, are plotted as a function of pH. (D) Ratios of the PE:PC, PE:APC, and PC:APC peak fluorescence intensities are plotted versus pH to help identify the dissociation pathways of the PBSomes.

a tendency to aggregate or precipitate. After incubation in a phosphate buffer lacking sucrose under different pH conditions, each PBSome sample is centrifuged at 20,000g to remove any full complexes remaining. The fluorescence emission is subsequently collected, with excitation at 480 nm, where only distal PE hexamers can be excited. As shown in Figure 4.11A, the emission scans of the supernatant shows an overall increase in fluorescence as the pH decreases. The latter is possibly due to an increase in solubility of dissociating subunits away form the APC. The normalization of the raw data clearly shows a shift in fluorescence away from the PE and towards PC subunits as the pH decreases (Figure 4.11B). All three measurable parts of these PBSomes increase in fluorescence with decreasing pH (Figure 4.11C). Figure 4.11D displays the ratios of the fluorescence of the measured subunits to one another to identify how these subunits change with respect to one another.

Chapter 5: Discussion and Conclusion

1. CpcG2-PSI Fusion

CpcG2 has been successfully modified to include flanking RsrII restriction sites and various spacers. Likewise, PsaX has also been successfully modified to have an RsrII restriction site for CpcG2 ligation and a kanamycin resistance gene inserted downstream of the PsaX gene. Ligation of these two products has been attempted, but met with either failed attempts or mutations in the fusion sequence. Aside from the failed ligation attempts resulting in the absence of transformant colonies, the most common problem faced is a truncation of the RsrII restriction site (Figure 5.1):

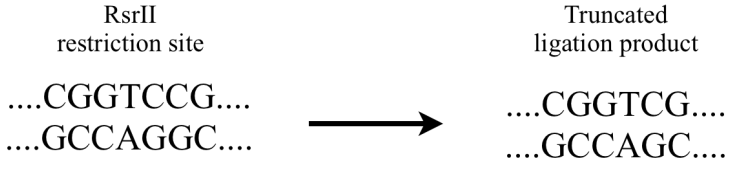


Figure 5.1: Mutation of the RsrII Restriction Site. After digestion with RsrII and subsequent ligation, an error in the plasmid product occured and is detected via sequencing. This change causes the loss of the RsrII restriction site and a frameshift mutation.

On rare occasion, after ligation and transformation, a few colonies formed, which, after culturing, plasmid purification, and sequencing, revealed a loss of the RsrII restriction site, regardless of whether the CpcG2 gene successfully inserted or

not. The truncation observed is a loss of a single base pair resulting in the loss of the restriction site and a frame-shift mutation. If this truncation results from the restriction digest, it can lead to a failure in the subsequent ligation and transformation steps. In the instance of a successful transformation, this mutation is also typically encountered, but the cause of the latter is unclear. Restriction digestion with RsrII is limited to one hour, and immediately followed by gel electrophoresis, gel clean-up, and ligation as quickly as possible to minimize over-digestion and loss of the nucleic acids in the overhang. However, the problem persisted over multiple attempts, and the cause could not be identified. Future studies will require an investigation into this problem.

2. Phycobilisome Dissociation

In the pursuit to find the appropriate conditions for the dissociation of PBSome rods from the core, three different methods are chosen. NaCl and urea are chaotropic agents used to dissociate the PBSome complex by disrupting electrostatic and hydrogen bonding interactions, respectively. Low-phosphate buffer conditions are also tested to monitor the dissociation pathways and rates of dissociation of PBSomes. Lastly, pH changes are made to alter the ionization states of the PBSome subunits, with the expectation that binding affinities will consequently be affected. Various PBSomes from different organisms are thus tested to provide a basis of comparison and insight into the PBSome complex dissociation. In particular, the results from the *Synechococcus* WH 8102 PBSome dissociation studies are of interest for the inclusion of its rods into the designed hydrogen evolution system.

Dissociation with NaCl provides some evidence of discrete rod formation, but only at the lowest concentrations of NaCl tested (i.e. below 0.2 M). In Figure 4.6D, an increase in the PC:APC ratio is observed, while the PE:PC ratio decreases slightly. Together, these ratios can be interpreted as rod formation in the absence of individual rod dissociation. The latter is reinforced by the normalized signals in Figure 4.6B, where a steady shift in fluorescence emissions away from the APC and towards the PC signal is observed. During this transition, the PE signal stagnates at roughly 80%, indicating that the dissociation of these rods does not occur. The PE signal remains stationary until a concentration of 0.2 M NaCl is reached, where the PE emission becomes the dominant fluorescing subunit. The latter indicates that these rods begin and continue to dissociate, and therefore no longer transfer energy to the PC or APC subunits. The raw signals also provide some interesting changes. From 0.2 - 0.6 M NaCl, the PE signal steadily increases, but the APC peak reduces to a shoulder as the PC signal concurrently increases in strength. The decrease in the APC signal indicates a decrease in energy transfer to the APC, which results from as discrete rod form. Above 0.6 M NaCl, the emission from all subunits decreases in intensity. This drop in intensity may be due to precipitation of the PBSomes caused by a salting-out effect due to high salt concentrations. The salt acts as a shield against water molecules, interrupting hydrogen bonding between the buffer and PBSomes, and thus results in a decrease in protein solubility.

Chaotropic studies with urea (Figure 4.7) provide similar results as NaCl, but with greater effectiveness in the dissociation of the PBSome complex. Again,

a shift in the fluorescence emission away from the APC towards the PC and a gradual increase in the PE signal is observed, indicating the separation of the PC from the APC core without rapid dissociation of individual PC rod subunits. Examination of the normalized values (Figure 4.7B) reveals that the PE signal does not actually increase with respect to the PC or the APC signal. Instead, the PE signal settles into one of three relative intensity ranges. At the lowest urea concentration (0.02 M), the PE emits at just under 40% (equivalent with the starting material) of the peak emission. From 0.04 M to 0.6 M urea, the normalized PE emission levels off at about 60% of the peak signal. Above 0.6 M urea, the PE signal increases again to be the dominant source of fluorescence. Interestingly, this trend reveals that the PE signal increases in steps rather than continuously as urea concentration increases. The same trend occurs in the NaCl studies, but only in a one-step increase in the normalized signal. The latter may be caused by a step-wise dissociation of the PE subunits away from the PBSome complex, and suggests that a threshold concentration of urea (or any chaotrope) is possibly needed to achieve targeted dissociation of the rods from the complex. Unfortunately, for this particular test, no concentration of urea seemed to elicit PC emissions, while keeping PE emissions minimized, indicating the inability to keep the whole rod intact.

Because high ionic strength is required to maintain its structure, PBSome dissociation under low-phosphate conditions is studied. Under low-phosphate low-ionic strength conditions, the PBSomes from *Synechocystis* PCC 6803 dissociate into individual subunits as shown in Figure 4.8. From 450 mM to 50

mM phosphate, faster changes in fluorescence occur as the complex dissociates with weaker ionic strengths of the buffer. Under these conditions, the PC signal increases with time and the APC emission concomitantly decreases. This inverse signal change signifies the decoupling of the PC-APC interface. Due to limitations of the stopped-flow machine, dissociation above 450 mM phosphate could not be examined with accuracy.

The low-phosphate dissociation studies of PBSomes from *Synechococcus* WH 8102 similarly measure the changes in the PE, as well as the PC and APC subunits (Figure 4.9). Initial results at the lowest phosphate concentrations show a rapid dissociation of the entire complex, as indicated by the dramatic increase in the PE signal, while both the PC and APC signals decrease in fluorescence. As the phosphate concentration increases, the rates of change for the three measured wavelengths slow as the PBSome complex dissociation slows. The PC signal, in particular, shows the most interesting changes because the signal did not simply slow its decline, but actually increased briefly, which indicates a short period in which the separation of the PC and APC occurs faster than the separation of the PE from the PC subunit. At 150 mM phosphate (Figure 4.9B), an increase in the PC signal is observed at the beginning of the scan before it reverts to a decrease. This trend not only continues, but becomes more prominent as phosphate concentration increases, which is explained by the dissociation of the rod from the APC core. Since the interruption of energy transfer between the PC to APC subunits results in the PC fluorescence, the increase in signal demonstrates that this dissociation step is the faster than the

dissociation of the PE from the PC subunit. The latter may provide a window of opportunity for the isolation of the PBSome rods by quenching its dissociation activity via the addition of high phosphate.

The pH-dependent dissociation of PBSomes in phosphate buffer is also investigated by fluorescence. As displayed in Figure 4.10, all samples show a blue shift in emission with decreasing pH, which results in an increase in the PC fluorescence because energy is no longer being transferred to the ACP core due to its dissociation from the complex. Peak emissions from PBSomes isolated from *Synechocystis* PCC 6803 and *T. elongates* BP-1 show the least change in fluorescence above pH 6.5, but exhibit a significant shift at pH 6. PBSomes from *Chroococcidiopsis* TS-821 show greater pH dependence than the former, exhibiting a blue shift starting below pH 7.5. Based on this data, whether or not the PC-containing rods are dissociating into individual hexamers or even smaller pieces is unclear. These tests serve as a quick precursor to study of the pH-dependent dissociation of PBSomes isolated from *Synechococcus* WH 8102.

In pH dissociation studies of PBSomes isolated from *Synechococcus* WH 8102 (Figure 4.11), the PE signal is initially relatively large in comparison to the PC and APC signals, which demonstrates the pH-independent dissociation of the PE subunits away from the rest of the rod structure. As the pH decreases from 7.8, the PC and APC signals sharply increase relative to PE, such that by pH 7.68, the PC signal appears to match the PE signal, as illustrated in the normalized graph (Figure 4.11B). The rise in the PC with respect to the PE signal is indicative of the liberation of the PBSome rods from the APC core, and

also implies that the rod itself is stable. Thus, the terminal PC hexamer that once transferred energy to the APC is now accepting energy from the distal PE subunits and fluorescing. If the individual rods had dissociated, the excited PE subunits would have fluoresced rather than transfer energy to the PC rods. The rise in the APC signal, however, may be either the result of its increased solubility with the decreased pH, or perhaps represent lower density PBSome complexes that have lost most, but not all of their rods. As the pH continues to decrease from 7.68, the PE begins to drop relative to the PC signal, and at the same time, the APC signal starts to increase. By pH 7.32, the PE signal is at its lowest in relation to the PC signal. These changes in intensities demonstrate a steady formation of PC rods from the APC core without the subsequent dissociation of the rods into individual pieces. As the pH is decreased further from 7.32, the PE signal resurges along with a decline in the APC signal. The latter may represent the beginning of the end for the liberation of rod structures, as the increase in the PE fluorescence invariably signifies a decrease in energy transfer to the PC and/or APC subunit. The accompanying decrease in the APC signal may be due to an increase, or perhaps more complete, dissociation of the PC from the APC subunit. Below pH 6.67, a dramatic increase in the PE signal and an equal decrease in PC signal representing the complete dissociation of the PBSome complex are likely to occur. In total, this last experiment shows the greatest chance to isolate rods from whole PBSome complex with minimal damage of the rod itself. The increase in the PC signal combined with the lack of an equally increasing PE emission is a very promising sign of rod formation.

3. Conclusion and Future Directions

The aim of this study is to create a PSI-CpcG2 fusion and isolate PBSomes rods for the increased efficiency of hydrogen evolution by greater light capture. The preliminary work to isolate and modify the requisite genes for the fusion is complete (with the exception of PsaK). Further work is required to fuse the CpcG2 gene with various spacer lengths to PsaX, as an unexpected truncation of the RsrII site in the ligation of the two pieces has caused problems and its prevention must be addressed. A possible solution to this problem is to perform an extra round of PCR with a new set of primers to edit-in the missing nucleic acid pair.

Targeted dissociation of the rod-APC interface is an interesting challenge. The intermolecular forces between these hexameric subunits are a combination of hydrophobic and electrostatic interactions that differ in strength. The results from this study reveal a potential path toward rod isolation from purified PBSomes using phosphate buffers at a specific pH. For *Synechococcus* WH 8102, clear rod dissociation from the core results at the pH range from 7 to 7.2. Future work will require the further separation of the PC rods from independent PE hexamers and APC complexes. As a precaution, the failure of the APC component to fluoresce simply means it is not receiving energy rather than indicate its absence. Additionally, FNR_L may still be attached to isolated rods, and a method to remove this impurity must be developed. Upon successful incorporation of the isolated rods to the designed fusion, the potential to increase the *in vitro* hydrogen evolution capabilities of the current system will be met.

Bibliography

Adir, N. (2003). "The Crystal Structure of a Novel Unmethylated Form of C-phycocyanin, a Possible Connector Between Cores and Rods in Phycobilisomes." Journal of Biological Chemistry **278**(28): 25926-25932.

Adir, N. (2005). "Elucidation of the molecular structures of components of the phycobilsiome: reconstructing a giant." Photosynthesis Research **85**: 15-32.

Adir, N., M. Dines, et al. (2006). Assembly and Disassembly of Phycobilisomes, Springer-Verlag.

Ajlani, G., C. Vernotte, et al. (1995). "Phycobilisome core mutants of *Synechocystis* PCC 6803." Biochimica et Biophysica Acta (BBA) **1231**(2): 189-196.

Allen, J. F. (2003). "State transitions - a question of balance." Science **299**: 1530-1532.

Anderson, L. K., M. C. Rayner, et al. (1984). "Ultra-violet mutagenesis of *Synchocystis* sp. 6701: utations in chromatic adaptation and phycobilisome assembly." Archives of Microbiology **138**: 237-243.

Anderson, S. L. and L. McIntosh (1991). "Light-activated heterotrophic growth of the cyanobacterium *Synechocystis* sp. strain PCC 6803: a blue-light-requiring process." Journal of Bacteriology **173**(9): 2761-2767.

Asada, K. (1994). "Production and action of active oxygen species in photosynthetic tissues." *In* C.H. Foyer and P. M. Mullineaux (ed.), Causesof photooxidative stress and amelioration of defense systems in plants. CRC Press, Boca Raton, FL: 77-104.

Ashby, M. K. and C. W. Mullineaux (1999). "The role of ApcD and ApcF in energy transfer from phycobilisomes to PSI and PSII in a cyanobacterium." Photosynthesis Research(61): 169-179.

Biggins, B. (1985). "Mechanism of the light-state transition in photosynthesis. V.

77K linear dichroism of *Anacystis nidulans* in state 1 and state 2." Biochemica et Biophysica Acta **810**: 295-301.

Brahamsha, B. (1996). "A genetic manipulation system for oceanic cyanobacteria of the genus *synechococcus*." Applied and environmental microbiology **62**(5): 1747-1751.

Brown, J. S. (1983). "A new evaluation of chlorophyll absorption in photosynthetic membranes." Photosynthesis Research **4**(4): 375-383.

Bryant, D. A., G. Guglielmi, et al. (1979). "The structure of cyanobacterial phycobilisomes: A model." Archives of Microbiology **123**: 113-127.

Busch, A., J. Nield, et al. (2010). "The composition and structure of photosystem I-associated antenna from Cyanidioschyzon merolae." The Plant Journal **62**(5): 886-897.

Campbell, L. and R. Iturriaga (1988). "Identification of *Synechococcus* spp. in the Sargasso Sea by immunofluorescence and fluorescence excitation spectroscopy performed on idividual cells." Limnology and Oceanography **33**(5): 1196-1201.

Capuano, V., A.-S. Braux, et al. (1991). "The "anchor polypeptide" of cyanobacterial phycobilisomes." The Journal of Biological Chemistry **266**(11): 7239-7247.

Chauvat, F., L. Vries, et al. (1986). "A host-vecto system for gene cloning in the cyanobacterium *Synechocystis* PCC 6803." Molecular Genetics and Genomics **204**(1): 185-191.

Conley, P. B., P. G. Lemaux, et al. (1988). "Molecular Characterization and evolution of sequences encoding light-harvesting components in the chromatically adapting cyanobacterium *Fremyella diplosiphon*." Journal of Molecular Biology **199**: 447-465.

Das, D. and T. N. Veziroğlu (2001). "Hydrogen production by biological processes: a survey of literature." International Journal of Hydrogen Energy **26**(1): 13-28.

David, L., A. Marx, et al. (2011). "High-Resolution Crystal Structures of Trimeric and Rod Phycocyanin." Journal of Molecular Biology **405**(1): 201-213.

Dong, C., A. Tang, et al. (2009). "ApcD is necessary for efficient energy transfer from phycobilisomes to photosystem I and helps to prevent photoinhibition in the cyanobacterium Synechococcus sp. PCC 7002." Biochimica et Biophysica Acta (BBA) - Bioenergetics **1787**(9): 1122-1128.

Edwards, M. R. and E. Gantt (1971). "Phycobilisomes of the thermophylic blue-green alga *Synechococcus lividus*." Journal of Cell Biology **50**: 896-900.

Everroad, C., C. Six, et al. (2006). "Biochemical Bases of Type IV Chromatic Adaptation in Marine Synechococcus spp." Journal of Bacteriology **188**(9): 3345-3356.

Frankenberg, N. and C. Lagarias (2003). "Phycocyanobilin:Ferredoxin Oxidoreductase (PcyA) of Anabaena sp. PCC 7120." JBC.

Fromme, P. (2001). "Structure of Photosystem I." Biochimica et Biophysica Acta (BBA)(1507): 5-31.

Fujimori, T., Y. Hihara, et al. (2005). "PsaK2 Subunit in Photosystem I is Involved in State Transition under High Light Conditon in the Cyanobacterium Synechocystis sp. PCC 6803." Journal of Biological Chemistry **280**(June 10): 22191-22197.

Gantt, E. (1996). "Pigment protein complexes and the concept of the photosynthetic unit: Chlorophyll complexes and phycobilisomes." Photosynthesis Research **48**: 47-53.

Gantt, E. and S. F. Conti (1965). "The ultrastructure of *Porphyridium cruentum*." Journal of Cell Biology **26**: 365-381.

Gingrich, J. C., D. J. Lundell, et al. (1983). "Core substructure in cyanobacterial phycobilisomes." Journal of Cellular Biochemistry **22**(1): 1-14.

Glazer, A. N. (1984). "Phycobilisome: a macromolecular complex optimized for light energy transfer." Biochimica et Biophysica Acta (BBA) **768**(1): 29-51.

Grossman, A., M. R. Schaefer, et al. (1993). "The phycobilisome, a light-harvesting complex responsive to environmental conditions." Microbiological Reviews **57**(3): 725-749.

Grossman, A. R., M. R. Schaefer, et al. (1993). "Environmental effects on the light-harvesting complex of cyanobacteria." Journal of Bacteriology **175**(3): 575-582.

Grotjohann, I. and P. Fromme (2005). "Structure of Cyanobacterial Photosystem I." Photosynthesis Research(85): 51-72.

Haldrup, A., P. E. Jensen, et al. (2001). "Balance of power: a view of the mechanism of photosynthetic state transitions." Trends in Plant Science **6**(7): 301-305.

Hatefi, Y. and W. Hanstein (1974). "Destabilization of membranes with chaotropic ions." Methods in Enzymology **31**: 770-790.

Hirose, Y., T. Shimada, et al. (2008). "Cyanobacteriochrome CcaS is the green light receptor that induces the expression of phycobilisome linker protein." Proceedings of the National Academy of Sciences **105**(28): 9528-9533.

Hossain, S., A. Salleh, et al. (2008). "Biodiesel fuel production from algae as renewable energy." American Journal of Biochemistry and Biotechnology **4**(3): 250-254.

Ishida, T., N. Hasegawa, et al. (1997). "Growth characteristics and dense culture of a thermophilic cyanobacterium, *Chroococcdiopsis* sp. strain TS-821." Journal of Fermentation and Bioengineering **83**(6): 571-576.

Iwuchukwu, I. J., M. Vaughn, et al. (2009). "Self-organized photosynthetic nanoparticle for cell-free hydrogen production." Nature Nanotechnology.

Jordan, P., P. Fromme, et al. (2001). "Three-dimensional structure of cyanobacterial photosystem I at 2.5 Angstrom resolution." Nature **411**:

909-917.

Kehoe, D. M. and A. Gutu (2006). "Responding to color: the regulation of complementary chromatic adaptation." Annual Review Compilations: Plant Physiology **57**(127-150).

Kohchi, T., K. Mukougawa, et al. (2001). "The *Arabidopsis* HY2 gene encodes phytochromobilin synthase, a ferredoxin-dependent biliverdin reductase." The Plant Cell **13**: 425-436.

Kondo, K., X. X. Geng, et al. (2005). "Distinct roles of CpcG1 and CpcG2 in phycobilsiome assembly in the cyanobacterium Synechocystis sp. PCC 6803." Photosynthesis Research **84**: 269-273.

Kondo, K., Y. Ochiai, et al. (2007). "The Membrane-Associated CpcG2-Phycobilisome in Synechocystis: A New Photosystem I Antenna." Plant Physiology **144**(2): 1200-1210.

Korn, A., G. Ajlani, et al. (2009). "Ferredoxin:NADP+ Oxidoreductase Association with Phycocyanin Modulates Its Properties." Journal of Biological Chemistry **284**(46): 31789-31797.

Liu, L.-N., X.-L. Chen, et al. (2005). "Characterization, structure and function of linker polypeptides in phycobilisomes of cyanobacteria and red algae: An overview." Biochimica et Biophysica Acta (BBA) - Bioenergetics **1708**(2): 133-142.

Liu, S., Y. Chen, et al. (2010). "Biosynthesis of fluorescent cyanobacterial allophycocyanin trimer in Escherichia coli." Photosynthesis Research **105**(2): 135-142.

Lloyd, B. and S. Subbarao (2009). "Development challenges under the Clean Development Mechanism (CDM) - Can renewable energy initiatives be put in place before peak oil?" Energy Policy **37**(1): 237-245.

MacColl, R. (1998). "Cyanobacterial Phycobilisomes." Journal of Structural Biology(124): 311-334.

MacColl, R. (2004). "Allophycocyanin and energy transfer." Biochimica et Biophysica Acta (BBA) - Bioenergetics **1657**(2-3): 73-81.

Mant, A. (2001). "Insertion of PsaK into the Thylakoid Membrane in a "Horseshoe" Conformation Occurs in the Absence of Signal Recognition Particle, Nucleoside Triphosphates, or Functional Albino3." Journal of Biological Chemistry **276**(39): 36200-36206.

Morris, I. and H. E. Glover (1981). "Physoilogy of photosynthesis by marine coccoid cyanobacteria - some ecological implications." Limnology and Oceanography **26**: 957-961.

Mullineaux, C. W. (1992). "Excitation energy transfer from phycobilsiomes to photosystem I in a cyanobacterium." Biochemica et Biophysica Acta **1100**: 285-292.

Mullineaux, C. W. (1994). "Excitation energy transfer from phycobilsiomes to photosystem I in a cyanobacterial mutant lacking photosystem II." Biochemica et Biophysica Acta **1184**: 71-77.

Mullineaux, C. W. (2007). "Phycobilisome-reaction centre interaction in cyanobacteria." Photosynthesis Research **95**(2-3): 175-182.

Mullineaux, C. W. and A. R. Holzwarth (1993). "Effect of photosystem II reaction centre closure on fluorescence decay kinetics in a cyanobacterium." Biochemica et Biophysica Acta **1183**: 345-351.

Naithani, S., J.-M. Hou, et al. (2000). "Targeted Inactivation of the psaK1, psaK 2, and psaM genes encoding subunits of Photosystem I in the cyanobacteriam Synechocystis sp. PCC 6803." Photosynthesis Research(63): 225-236.

Olive, J., G. Ajlani, et al. (1997). "Ultrastructure and light adaptation of phycobilisome mutants of *Synechocystis* PCC 6803." Biochemica et Biophysica Acta **1319**: 275-282.

Ong, L. J. and A. N. Glazer (1991). "Phycoerythrins of marine unicellular cyanobacteria. I. Bilin types and locations and energy transfer pathways in *Synechococcus* spp. phycoerythrins." JBC **266**: 9515-9527.

Padyana, A. K., V. B. Bhat, et al. (2001). "Crystal Structure of a Light-Harvesting Protein C-Phycocyanin from Spirulina platensis." Biochemical and Biophysical Research Communications **282**(4): 893-898.

Parbel, A. and H. Scheer (2000). "Model for the phycobilisome rod with interlocking disks based on domain-weighted linker-polypeptide sequence homologies of *Mastigocladus laminosus*." International Journal of Photoenergy **2**: 31-40.

Pimentel, D. (1991). "Ethanol fuels: Energy security, economics, and the environment." Journal of Agricultural and Evironmental Ethics **4**(1): 1-13.

Pizarro, S. A. and K. Sauer (2001). "Spectroscopic study of the light harvesting protein C0phycocyanin associated with colorless linker peptides." Photochemistry and Photobiology **73**(5): 556-563.

Reuter, W., G. Wiegand, et al. (1999). "Structural analysis at 2.2Å of orthorhombic crystals presents the asymmetry of the allophycocyanin-linker complex AP·LC7.8, from phycobilisomes of *Mstigocladus laminosus*." Proceedings of the National Academy of Sciences **96**: 1363-1368.

Rogner, M., U. Miihlenhoff, et al. (1990). "Mono-, di-, and trimeric PS I reaction center complexes isolated from the thermophilic cyanobacterium *Synechococcus* sp. * Size, shape and activity." Biochemica et Biophysica Acta **1015**: 415-424.

Scheer, H. and K. H. Zhao (2008). "Biliprotein maturation: the chromophore attachment." Molecular Microbiology **68**(2): 263-276.

Schubert, W.-D., O. Klukas, et al. (1997). "Photosystem I of *Synechococcus elongatus* at 4 angstrom resolution: comprehensive structural analysis." Journal of Molecular Biology **272**: 741-769.

Sidler, W. (1994). "Phycobilsiome and phycobiliprotein structures." The Molecular Biology of Cyanobacteria: 139-216.

Singh, A. K., M. Bhattacharyya-Pakrasi, et al. (2009). "A Systems-Level Analysis of the Effects of Light Quality on the Metabolism of a Cyanobacterium." Plant Physiology **151**(3): 1596-1608.

Six, C., J.-C. Thomas, et al. (2007). "Diversity and evolution of phycobilisomes in marine Synechococcus spp.: a comparative genomics study." Genome Biology **8**(12): R259.

Six, C., J. C. Thomas, et al. (2005). "Two Novel Phycoerythrin-Associated Linker Proteins in the Marine Cyanobacterium Synechococcus sp. Strain WH8102." Journal of Bacteriology **187**(5): 1685-1694.

Stec, B., R. F. Troxler, et al. (1999). "Crystal structure of C-phycocyanin from Cyanidium caldarium provides a new perspective on phycobilisome assembly." Biophysical Journal **76**(June): 2912-2921.

Takakazu, K., S. Sato, et al. (1996). "Sequence analysis of the genome of the unicellular cyanobacterium *Synechocystis* sp. strain PCC6803. II. Sequence determination of the entire genome and assignment of potential protein-coding regions." DNA research **3**(3): 109-136.

Tandeau de Marsac, N. and G. Cohen-Bazire (1977). "Molecular composition of cyanobacterial phycobilisomes." Proceedings of the National Academy of Sciences(74): 1635-1639.

Tilman, D., J. Hill, et al. (2006). "Carbon-Negative Biofuels from low-input high-diversity grassland biomass." Science **314**: 1598-1600.

Toole, C. M., T. L. Plank, et al. (1998). "Bilin deletions and subunit stability in cyanobacterial light-harvesting proteins." Molecular Microbiology **30**(3): 475-486.

Walters, R. G. (2005). "Towards an understanding of photosynthetic acclimation." Journal of Experimental Botany **56**: 435-447.

Wollman, F.-A. (2001). "State transitions reveal the dynamics and flexibility of the photosynthetic apparatus." The EMBO Journal **20**: 3623-3630.

Xu, h., D. Vavilin, et al. (2004). "Multiple deletions of the small cab-like proteins in the cyanobacterium *Synechocystis* sp. PCC 6803. Consequences for pigment biosynthesis and accumulation." Journal of Biological Chemistry **279**: 27971-27979.

Yang, S., R. Zhang, et al. (2009). "The dynamic behavior of phycobilisome movement during light state transitions in cyanobacterium Synechocystis PCC6803." Photosynthesis Research **99**(2): 99-106.

Zilinskas, B. and R. E. Glick (1981). "Noncovalent intermolecular forces in phycobilisomes of *Porphyridium cruentum*." Plant Physiology **68**: 447-452.

Appendices

Appendix 1: Amino Acid Length, MW, and pI of Phycobilisome Proteins

Organism/Gene Name	Gene Product	Amino Acid Length	MW (Da)	pI
Synechocystis sp. PCC 6803				
apcA	allophycocyanin alpha subunit	161	17411.83	4.86
apcB	allophycocyanin beta subunit	161	17215.64	5.43
apcC	L_C linker	67	7805.16	10.94
apcD	allophycocyanin α^B (alpha substitute)	161	17932.45	5.44
apcE	L_{CM} linker	896	100295.87	9.25
apcF	allophycocyanin B^{18} (beta substitute)	169	18892.45	4.96
cpcA	phycocyanin alpha subunit	162	17586.60	5.35
cpcB	phycocyanin beta subunit	172	18126.47	4.98
cpcG1	L_{RC} rod-core linker	249	28901.78	9.34
cpcG2	L_{RC} rod-core linker	249	28522.59	9.14
cpcC1	L_R rod linker	291	32520.67	9.35
cpcC2	L_R rod linker	273	30797.38	9.39
cpcD	L_R rod capping linker	83	9322.35	9.39

Organism/Gene Name	Gene Product	Amino Acid Length	MW (Da)	pI
Thermosynechococcus elongatus BP-1				
apcA	allophycocyanin alpha subunit	161	17538.96	4.85
apcB	allophycocyanin beta subunit	161	17358.89	5.45
apcC	L_C linker	67	7864.25	10.44
apcD	allophycocyanin α^B (alpha substitute)	171	19228	4.97
apcE	L_{CM} linker	1139	127612.25	9.39
apcF	allophycocyanin B^{18} (beta substitute)	169	18723.23	5.27
cpcA	phycocyanin alpha subunit	162	17442.7	5.36
cpcB	phycocyanin beta subunit	172	18186.67	5.12
cpcG1	L_{RC} rod-core linker	277	31624.15	9.74
cpcG2	L_{RC} rod-core linker	246	28779.39	9.34
cpcG4	L_{RC} rod-core linker	251	29585.53	9.28
cpcC	L_R rod linker	287	32123.98	6.77
cpcD	L_R rod capping linker	78	8671.91	10.21

Appendix 1: Amino Acid Length, MW, and pI of Phycobilisome Proteins (cont.)

Organism/Gene Name	Gene Product	Amino Acid Length	MW (Da)	pI
Synechococcus sp. WH7803				
apcA	allophycocyanin alpha subunit	161	17374.8	4.76
apcB	allophycocyanin beta subunit	162	17440.78	4.89
apcC	L_C linker	66	7743.95	10.03
apcD	allophycocyanin α^B (alpha substitute)	164	18304.99	5.02
apcE	L_{CM} linker	979	107149.8	9.76
apcF	allophycocyanin B^{18} (beta substitute)	174	19366.11	5.14
rpcA	R-phycocyanin II alpha subunit	162	17320.38	5.14
rpcB	R-phycocyanin II beta subunit	172	17909.26	5.10
cpeA	C-phycoerythrin I alpha subunit	164	17796.11	5.46
cpeB	C-phycoerythrin I beta subunit	184	19058.67	5.82
mpeA	C-phycoerythrin II alpha subunit	165	17824.96	5.83
mpeB	C-phycoerythrin II beta subunit	181	18700.17	5.37
cpcG1	L_{RC} rod-core linker	252	28497.35	9.51
cpcG2	L_{RC} rod-core linker	243	27787.39	7.78
cpeC	L_R C-phycoerythrin I associated rod linker	294	33173.12	7.75
cpeE	L_R C-phycoerythrin I associated rod linker	245	26958.09	8.73
mpeD	L_R C-phycoerythrin II associated rod linker	546	59158.92	8.24
mpeE	L_R C-phycoerythrin II associated rod linker	286	31156.25	8.90

Appendix 1: Amino Acid Length, MW, and pI of Phycobilisome Proteins (cont.)

Organism/Gene Name	Gene Product	Amino Acid Length	MW (Da)	pI
Synechococcus sp. WH8102				
apcA	allophycocyanin alpha subunit	161	17371.85	4.74
apcB	allophycocyanin beta subunit	162	17463.82	4.89
apcC	L_C linker	66	7713.93	10.03
apcD	allophycocyanin α^B (alpha substitute)	164	18145.98	5.00
apcE	L_{CM} linker	963	104989.29	9.44
apcF	allophycocyanin B^{18} (beta substitute)	174	19328.04	5.31
rpcA	R-phycocyanin II alpha subunit	162	17335.44	6.10
rpcB	R-phycocyanin II beta subunit	172	17975.33	5.08
cpeA	C-phycoerythrin I alpha subunit	164	17817.09	5.45
cpeB	C-phycoerythrin I beta subunit	184	19146.77	6.25
mpeA	C-phycoerythrin II alpha subunit	165	17728.96	7.64
mpeB	C-phycoerythrin II beta subunit	178	18084.53	5.36
CpcG1	L_{RC} rod-core linker	252	28372.30	8.94
CpcG2	L_{RC} rod-core linker	252	28101.08	5.83
cpeC	L_R C-phycoerythrin I associated rod linker	252	31953.03	6.38
mpeC	L_R C-phycoerythrin II associated rod linker (gamma linker unit)	293	31953.03	9.03
mpeD	L_R C-phycoerythrin II associated rod linker	548	59408.68	8.97
mpeE	L_R C-phycoerythrin II associated rod linker	300	32804.81	9.06

Appendix 2: Chaotrope Assay Design

Desired Chaotrope Concentration (M)	Sample Volume (µL)	Amount of 3M Chaotrope (µL)	Additional 750mM phosphate buffer (µL)
0	10	0	90
0.02	10	0.66	89.33
0.04	10	1.33	88.66
0.06	10	2	88
0.08	10	2.66	87.33
0.1	10	3.33	86.66
0.2	10	6.66	83.33
0.4	10	13.33	76.66
0.6	10	20	70
0.8	10	26.66	63.33
1	10	33.33	56.66
1.5	10	50	40
2	10	66.66	23.33

Appendix 3: Media Recipes

A+ Medium

For 1L media

Part A	500 ml
Part B	500 ml

Autoclave

Vitamin solution (10,000x)	250 µl/l
A+ Trace metals (4000x)	100 µl/l

Parts A and B are to be made and autoclaved separately. When cool, combine into sterile 1 liter bottle and add vitamin solution and A+ trace metals

Part A	mg/l
NaCl	18,000
$MgSO_4 \cdot 7H_2O$	5000
KCl	600
H_3BO_3	40
$CaCl_2 \cdot 2H_2O$	360

Part B	mg/l
Na_2EDTA	30
KH_2PO_4	50
$NaNO_3$	1000
Tris	605
$FeCl_3$	1ml

Vitamin solution (10,000x)	Mg/ml
Thiamine	100
Vitamin B_{12}	2
Biotin	1

A+ Trace metals (4000x)	mg/l
$CuSO_4$	10
$ZnSO_4$	22
$CoCl_2$	10
$MnCl_2 \cdot 4H_2O$	180
$NaMoO_4$ $2H_2O$	6

ASN Medium

Turks Island Salt Mix	1000 ml

Autoclave

NaEDTA (1000x)	1ml/l
K_2HPO_4 (1000x)	1ml/l
$NaNO_3$ (100x)	10ml/l
Cyano trace metals (1000x)	1ml/L
Vitamin solution (10,000x) (same as A+)	100ul/l

Make Turk's Island Salt Mix, autoclave and add ASN stock solutions, trace metals and vitamin solutions when cooled.

Turks Island Salt Mix	mg/l
NaCl	28,100
$MgSO_4 \cdot 7H_2O$ ($MgSO_4$ anhydrous)	6900 (3450)
$MgCl \cdot 6H_2O$	5490
KCl	670
$CaCl \cdot 2H_2O$	1470

$Na_2EDTA \cdot 2H_2O$ (1000X)	5.58 g/l

K_2HPO_4 (1000X) (anhydrous)	15.7 g/l

$NaNO_3$ (100x)	78.0 g/l

Cyano trace metals	mg/l
Citric acid $\cdot H_2O$	6250
Ferric ammonium citrate	6000
$MnCl_2 \cdot 4H_2O$	1400
$Na_2MoO_4 \cdot 2H_2O$	390
$Co(NO_3)_2 \cdot 6H_2O$	25
$ZnSO_4 \cdot 7H_2O$	222

Appendix 4: Primers

CpcG2 Primers

Red: Restriction site

Orange: Ser-Ser-Gly spacer encoding sequence

Primer Name	Sequence
CpcG2 Forward	GGTGGTCGGTCCGCATGGCCCTCCCGCTCCTCG
CpcG2 0-link Reverse	GGTGGTCGGACCGCGGTCTCCAGCTGTTGCATCTGAG
CpcG2 1-link Reverse	GGTGGTCGGACCGCGCCGCCAGAGGTCTCCAGCTGTTGCATCTGAG
CpcG2 2-link Reverse	GGTGGTCGGACCGCGCCGCCACTGCCGCCAGAGGTCTCCAGCTGTTGCATCTGAG
CpcG2 3-link Reverse	GGTGGTCGGACCGCGCCGCCACTGCCGCCACTGCCGCCAGAGGTCTCCAGCTGTTGCATCTGAG

PsaX Primer

Primer Name	Sequence
PsaX-CpcG2_F	GCCGTTTCCTACGGTCCGCATGGCCCTCCCGCTCCTC
PsaX-CpcG2_R	
PsaX HindIII fw r2	TCAAGTAGGACTTGAAGCTTAAGGATTGCGGAGGC
PsaX HindIII rv r2	GCCTCCGCAATCCTTAAGCTTCAAGTCCTACTTGA

PsaK Primers

Primer Name	Sequence
PsaK-CpcG2_F	
PsaK-CpcG2_R	
PsaK HindIII fw r2	GCCGGCGCCCTCTAGAAGCTTTTAGCCACTGGCAATCTG
PsaK HindIII rv r2	CAGATTGCCAGTGGCTAAAAGCTTCTAGAGGGCGCCGGC

Appendix 5: PCR conditions

1. Initial Denature	96	4 minutes
2. Denature	96	30 seconds
3. Anneal	X	30 seconds
4. Elongation	72	Y
Repeat steps 2-4 30 times		
5. Extended Elongation	72	1 minute
6. Stop	4	hold

X = 5 degrees below lowest primer melting temperature

Y = 1 minute per thousand bases

Vita

Paul Abraham Willard was born in Seoul South Korea on June 30, 1984. During his childhood as an army brat, he lived in multiple places, including Germany, Arizona, and Alabama. Upon his father's retirement from the army, Paul and his family moved to Massachusetts, and then moved with his family to Nashville, Tennessee, where he attended Lighthouse Christian School from 7th grade until he graduated in 2002. Paul attended the University of Tennessee, Knoxville as an undergraduate, where he received his bachelor's degree in microbiology in the fall of 2007. In his lasts semester as an undergrad, he joined Dr. Barry Bruce's lab, and after graduation, continued working as a lab technician. During this time, Paul accepted the opportunity to enroll as a graduate student in the chemical engineering department at UT Knoxville, where he received his master's degree in biomolecular engineering. THE END?